# HYDRUS

# WETLAND MODULE

## VERSION 2

Manual

by

Günter Langergraber[1] and Jirka Šimůnek[2]

March 2011

[1] Institute for Sanitary Engineering and Water Pollution Control
BOKU - University of Natural Resources and Life Sciences, Vienna
Muthgasse 18, A-1190 Vienna, Austria

[2] Department of Environmental Sciences
University of California Riverside
Riverside, CA, 92521, USA

**Abstract**

Langergraber, G. and J. Šimůnek, HYDRUS Wetland Module, Version 2. *Hydrus Software Series 4*, Department of Environmental Sciences, University of California Riverside, Riverside, California, USA, p. 56, 2011.

This report documents version 2 of the HYDRUS wetland module. In version 2, two biokinetic model formulations can be chosen: (1) CW2D (Langergraber and Šimůnek, 2005) and (2) CWM1 (Constructed Wetland Model #1) (Langergraber et al., 2009b). Aerobic and anoxic transformation and degradation processes for organic matter, nitrogen and phosphorus are considered in CW2D, whereas aerobic, anoxic and anaerobic processes for organic matter, nitrogen and sulphur are considered in CWM1.

**DISCLAIMER**

This report documents version 2 of the HYDRUS wetland module. The Wetland module was developed as a supplemental module of the HYDRUS software package, to model the biochemical transformation and degradation processes in subsurface wetlands. The software has been verified against selected test cases. However, no warranty is given that the program is completely error-free. If you do encounter problems with the code, find errors, or have suggestions for improvement, please contact one of the authors at

Günter Langergraber
Tel: +43-(0)1-47654-5814
Fax: +43-(0)1-368 99 49
Email: guenter.langergraber@boku.ac.at

Jirka Šimůnek
Tel/Fax: 1-951-827-7854
Email: jiri.simunek@ucr.edu

# Table of contents

# List of Figures

# List of Tables

# 1 Introduction

Constructed Wetlands (CWs) are engineered water treatment systems that optimize the treatment processes found in natural environments. CWs are popular systems which efficiently treat different kinds of polluted water and are therefore sustainable environmentally friendly solutions. A large number of physical, chemical and biological processes are simultaneously active and mutually influence each other (e.g., Kadlec and Wallace, 2009). As complex systems, CWs for a long time have been considered as "black boxes". Only little effort has been made to understand the main processes leading to contaminant removal. Only recently, efforts have been made to understand the processes in CWs in more detail, and modern tools from environmental microbiology, plant biology, ecology, and molecular biology have been used for this purpose (e.g., Faulwetter et al., 2009).

During the last few years, models of different complexities have been developed for describing processes in SubSurface Flow (SSF) CWs. The main objective of numerical modeling of CWs is to obtain a better understanding of the processes governing the biological and chemical transformation and degradation processes, to provide insights into these "black box" systems, and last but not least, to evaluate and improve existing design criteria (Langergraber, 2008).

This report documents version 2 of the HYDRUS wetland module. Version 2 of the HYDRUS wetland module includes two biokinetic model formulations: (1) the CW2D module (Langergraber and Šimůnek, 2005), and/or (2) the CWM1 (Constructed Wetland Model #1) biokinetic model (Langergraber et al., 2009b). In CW2D, aerobic and anoxic transformation and degradation processes for organic matter, nitrogen and phosphorus are described, whereas in CWM1, aerobic, anoxic and anaerobic processes for organic matter, nitrogen and sulphur are considered. CWM1 has been developed with the main goal to provide a widely accepted model formulation for biochemical transformation and degradation processes in SSF CWs. The HYDRUS wetland module is the only implementation of a CW model that is currently publicly available.

Chapter 2 gives a brief overview of available numerical models for SSF CWs. Chapter 3 describes the CW2D and CWM1 biokinetic models, whereas Chapter 4 describes their implementation into HYDRUS. Chapter 5 describes two additional examples: *Wetland 4* shows the startup of a simulation using the CWM1 biokinetic model and *Wetland 5* the simulation of the effects of wetland plants. A description of additional input and output files is then provided in Chapters 6 and 7, respectively.

For detailed information about the CW2D and CWM1 biokinetic models, the reader is referred to the original papers, i.e., Langergraber and Šimůnek (2005) and Langergraber et al. (2009b), respectively. For detailed information on how to set-up models for SSF CWs in HYDRUS, the reader is referred to the manual of version 1 of the HYDRUS wetland module (Langergraber and Šimůnek, 2006). For general information on HYDRUS the reader is referred to Šimůnek et al. (2008), for detailed information on the software to the technical manual (Šimůnek et al., 2011).

# 2 Modeling of constructed wetlands

## 2.1 Numerical models for SSF CWs

No free water level is visible in SSF CWs and water flows either horizontally or vertically through the porous filter media. Horizontal Flow (HF) systems can be simulated when only water flow saturated conditions are considered. A series or network of continuously stirred tank reactors (CSTRs) is most frequently used to describe the hydraulics of these systems, and reactions are modeled with various complexities. For modeling vertical flow (VF) CWs with intermittent loading, transient variably-saturated flow models are required. Due to the intermittent loading, these systems are highly dynamic, adding to the complexity needed to model the overall system. Models applicable to VF CWs use either the Richards equation or other simplified approaches to describe variably-saturated flow.

The following list (Langergraber, 2011) summarizes process-based numerical models available for subsurface flow CWs, whereby only models with minimum complexity in describing water flow and/or biochemical processes are listed. More information on the models can be found in recently published review papers (Langergraber, 2008, 2010; and Langergraber et al., 2009a) and in the original references, respectively.

1. *Complex flow models with transport of a single solute*
   - Schwager and Boller (1997): finite-element flow model, simulating tracer and oxygen transport in intermittent sand filters.
   - Forquet et al. (2009): two-phase flow numerical model (based on finite-elements), simulating the parallel movement of air and water in a VF filter.
2. *Reactive transport models for saturated flow conditions*
   - Reactive transport models applicable only for constant flow rates:
     - Mashauri and Kayombo (2002): only carbon transformation processes.
     - Mayo and Bigambo (2005): only nitrogen transformation processes.
     - Wang et al. (2009): only nitrogen transformation processes.
   - Reactive transport models with a tanks-in-series approach for water flow:
     - Chen et al. (1999): only carbon transformation processes.
     - Wynn and Liehr (2001): carbon and nitrogen transformation processes.
     - Marsili-Libelli and Checchi (2005): carbon and nitrogen transformation processes.
     - Rousseau (2005): carbon and nitrogen transformation processes; a reaction model in matrix notation based on the mathematical formulation of the Activated Sludge Models (ASMs; Henze et al., 2000).
   - Reactive transport models coupled to a complex groundwater flow model:
     - PHWAT (Brovelli et al., 2009a,b): carbon and nitrogen transformation processes; a reaction model in the matrix notation based on ASMs, coupled with the groundwater flow model MODFLOW; an extension of MODFLOW for unsaturated zones is on the way to be implemented.

3. *Reactive transport models for variably-saturated flow*
   - Reactive transport models with simplified approaches for simulating variably-saturated water flow:
     - McGechan et al. (2005): different horizontal layers to describe variably-saturated water flow; considers pools of organic matter, ammonium, nitrate and oxygen; microbiologically controlled transformations between these pools.
     - FITOVERT (Giraldi et al., 2010): different horizontal layers to describe variably-saturated water flow; a reaction model in the matrix notation based on ASMs describing carbon and nitrogen transformation processes, implemented in Matlab®.
     - Freire et al. (2009): combination of CSTRs and dead-zones to describe variably-saturated flow; description of the removal processes for the dye AO7 only.
   - Reactive transport models coupled with flow models that use the Richards equation to describe variably-saturated water flow:
     - CW2D (Langergraber, 2001; Langergraber and Šimůnek, 2005): implemented in the HYDRUS software; a reaction model in the matrix notation based on ASMs describing carbon, nitrogen, and phosphorous transformation processes, it has most published applications.
     - Ojeda et al. (2008): implemented in the RetrasoCodeBright (RCB) flow model, simplified description of organic matter, nitrogen, and sulphur transformation processes.
     - Wanko et al. (2006): considers organic matter removal and oxygen transport in VF filters.
     - Maier et al. (2009): implemented in the MIN3P flow and transport code; describes processes in CWs for the remediation of contaminated groundwater.

## 2.2 The Constructed Wetland Model N°1 (CWM1)

The Constructed Wetland Model N°1 (CWM1) is a general model describing biochemical transformation and degradation processes for organic matter, nitrogen, and sulphur in SSF CWs (Langergraber et al., 2009b). CWM1 has been published with the main goal to provide a widely accepted model formulation for biochemical transformation and degradation processes in CWs that can then be implemented in various simulation tools. CWM1 describes all relevant aerobic, anoxic, and anaerobic biokinetic processes occurring in HF and VF CWs that need to be considered in order to predict effluent concentrations of organic matter, nitrogen, and sulphur. 17 processes and 16 components (8 solute and 8 particulate components) are considered.

Version 2 of the HYDRUS wetland model provides the first available implementation of CWM1.

# 3 Description of the CW2D and CWM1 biokinetic models

## 3.1 Principles

In version 2 of the HYDRUS wetland module, two biokinetic models for describing the transformation and degradation processes are implemented:

1. CW2D (Langergraber and Šimůnek, 2005) was mainly developed for modeling VF systems and therefore includes only aerobic and anoxic transformation and degradation processes. These processes are described for the main constituents of wastewater, i.e., organic matter, nitrogen, and phosphorus.
2. CWM1 (Constructed Wetland Model #1, Langergraber et al., 2009b) was developed as a general model describing biochemical transformation and degradation processes for organic matter, nitrogen, and sulphur in HF and VF CWs. CWM1 describes all relevant aerobic, anoxic, and anaerobic biokinetic processes occurring in HF and VF CWs required to predict effluent concentrations of organic matter, nitrogen, and sulphur.

As the wastewater constituents considered in the CW2D and CWM1 biokinetic models are different, it has to be noted that no direct conversion between model components is possible and therefore provided by the HYDRUS GUI. The user is responsible for the correct use of the two biokinetic models.

## 3.2 Matrix format and notation

It is a common practice to present biokinetic models using the matrix notation introduced by the IWA (International Water Association) for ASMs (Henze *et al.*, 2000). The Gujer matrix consists of 3 parts representing:

1. stoichiometry,
2. kinetic rate expressions, and
3. composition.

A simple model representing aerobic heterotrophic bacteria growth and decay (adapted from Henze *et al.*, 2000) is chosen as an example to illustrate the use of the Gujer matrix. Table 3.1 describes two processes (growth and decay of heterotrophic bacteria) and three components (biomass, substrate, and dissolved oxygen). Bacteria need energy to integrate their carbon substrate and produce new biomass. Heterotrophs ($X_{OHO}$) find their energy and their carbon source in an organic substrate ($S_B$) and use dissolved oxygen ($S_{O2}$) as an electron acceptor under aerobic conditions. Consequently, only part of the substrate used by bacteria will directly contribute to biomass growth ($1/Y_{OHO}$), whereas the other part is oxidized to produce energy ($1-1/Y_{OHO}$).

In this example, the growth rate depends on the maximum growth rate of the heterotrophic biomass ($\mu_{OHO,Max}$), the biomass concentration ($X_{OHO}$), the availability of the substrate for the bacteria ($S_B/(K_{SB,OHO}+S_B)$ where $K_{SB,OHO}$ is the half-saturation coefficient for $S_B$), and the availability of electron acceptors ($S_{O2}/(K_{SO2,OHO}+S_{O2})$ where $K_{SO2,OHO}$ is the half-saturation coefficient for $S_{O2}$). The ratios $S_B/(K_{SB,OHO}+S_B)$ and $S_{O2}/(K_{SO2,OHO}+S_{O2})$ are the Monod equations used as a switching function for substrate, nutrients, alkalinity, and electron acceptors. Similarly, when a process occurs only when a component is absent (e.g., dissolved oxygen in anoxic processes), the switching function takes the following form: $K_{O2,OHO}/(K_{O2,OHO}+S_{O2})$ .

The continuity check for every process is calculated by multiplying the stoichiometric coefficients by the correlated term in the composition matrix for every component and summing up for different processes (recalling that oxygen is negative COD, its coefficient must thus be multiplied by -1).

Table 3.1: Gujer matrix describing process kinetics and stoichiometry for heterotrophic bacterial growth in an aerobic environment (adapted from Henze et al., 2000, using the notations of Corominas et al., 2010)

| **Continuity →** | Heterotrophic biomass (mg COD/L) | Substrate (mg COD/ L) | Dissolved oxygen (-mg COD/ L) | |
|---|---|---|---|---|
| Component (i) | 1 | 2 | 3 | Process rate $\rho_j$ |
| Process (j) ↓ Mass balance | $X_{OHO}$ | $S_B$ | $S_{O2}$ | |
| 1. Growth | 1 | $-\frac{1}{Y_{OHO}}$ | $-\frac{1-Y_{OHO}}{Y_{OHO}}$ | $\mu_{OHO,Max}\frac{S_B}{K_{SB,OHO}+S_B}\frac{S_{O2}}{K_{SO2,OHO}+S_{O2}}X_{OHO}$ |
| 2. Decay | -1 | | -1 | $b_{OHO}\ X_{OHO}$ |

Stoichiometric parameters: $Y_{OHO}$ = Heterotrophic yield coefficient

Kinetic parameters:
$\mu_{OHO,Max}$ = Maximum heterotrophic growth rate
$K_{SB,OHO}$ = Half-saturation coefficient for substrate
$K_{SO2,OHO}$ = Half-saturation coefficient for oxygen
$b_{OHO}$ = Heterotrophic decay rate

The reaction rates for the three components are calculated by summing up the products of the stoichiometric factor and the process rate over the different processes. For the example described above the reaction rates are calculated as follows:

$$
\begin{aligned}
r_{X_{OHO}} &= \mu_{OHO,max}\frac{S_B}{K_{SB,OHO}+S_B}\frac{S_{O2}}{K_{SO2,OHO}+S_{O2}}X_{OHO} - b_{OHO}X_{OHO} \\
r_{S_B} &= -\frac{1}{Y_{OHO}}\mu_{OHO,max}\frac{S_B}{K_{SB,OHO}+S_B}\frac{S_{O2}}{K_{SO2,OHO}+S_{O2}}X_{OHO} \\
r_{S_O} &= -\left(\frac{1-Y_{OHO}}{Y_{OHO}}\right)\mu_{OHO,max}\frac{S_B}{K_{SB,OHO}+S_B}\frac{S_{O2}}{K_{SO2,OHO}+S_{O2}}X_{OHO} - b_{OHO}X_{OHO}
\end{aligned}
\tag{3.1}
$$

## 3.3 Comparison of CW2D and CWM1 components and processes

Table 3.2 compares the components defined in the CW2D and CWM1 model formulations. As described before, both biokinetic models describe processes affecting organic matter and nitrogen. Additionally, CW2D also describes processes affecting phosphorus, whereas CWM1 describes processes affecting sulphur.

Table 3.2: Comparison of CW2D and CWM1 components.

| **CW2D** (Langergraber and Šimůnek, 2005) | **CWM1** (Langergraber et al., 2009b) |
|---|---|
| **Organic matter, nitrogen, phosphorus** | **Organic matter, nitrogen, sulphur** |
| **CW2D components**<br>1. **SO**: *Dissolved oxygen*, O2.<br>2. **CR**: *Readily biodegradable soluble COD.*<br>3. **CS**: *Slowly biodegradable soluble COD.*<br>4. **CI**: *Inert soluble COD.*<br>5. **XH**: *Heterotrophic bacteria*<br>6. **XANs**: *Autotrophic ammonia oxidizing bacteria (Nitrosomonas spp.)*<br>7. **XANb**: *Autotrophic nitrite oxidizing bacteria (Nitrobacter spp.)*<br>8. **NH4N:** *Ammonium and ammonia nitrogen*.<br>9. **NO2N:** *Nitrite nitrogen.*<br>10. **NO3N:** *Nitrate nitrogen*.<br>11. **N2:** *Elemental nitrogen.*<br>12. **PO4P:** *Phosphate phosphorus*<br><br>Organic nitrogen and organic phosphorus are modeled as part of the COD.<br>Nitrification is modeled as a two-step process.<br>Bacteria are assumed to be immobile.<br><br>It is generally assumed that all components except bacteria are soluble. | **Soluble components**<br>1. **SO**: *Dissolved oxygen*, O2.<br>2. **SF**: *Fermentable, readily biodegradable soluble COD*.<br>3. **SA**: *Fermentation products as acetate*.<br>4. **SI**: *Inert soluble COD*.<br>5. **SNH**: *Ammonium and ammonia nitrogen*.<br>6. **SNO**: *Nitrate and nitrite nitrogen.*<br>7. **SSO4**: *Sulphate sulphur*.<br>8. **SH2S**: *Dihydrogensulphide sulphur*.<br>**Particulate components**<br>9. **XS**: *Slowly biodegradable particulate COD.*<br>10. **XI**: *Inert particulate COD.*<br>11. **XH**: *Heterotrophic bacteria*.<br>12. **XA**: *Autotrophic nitrifying bacteria*.<br>13. **XFB**: *Fermenting bacteria*.<br>14. **XAMB**: *Acetotrophic methanogenic bacteria*.<br>15. **XASRB**: *Acetotrophic sulphate reducing bacteria*.<br>16. **XSOB**: *Sulphide oxidizing bacteria*.<br><br>Organic nitrogen and organic phosphorus are modeled as part of the COD. |

Contrary to version 1 of the HYDRUS wetland module, organic matter components are defined in both liquid and solid phases, i.e., adsorption/desorption processes of organic matter components can be modeled in version 2. Table 3.3 summarizes in what phases (i.e., liquid and/or solid) the CW2D and CWM1 components are defined. It has to be noted that the number of components in Table 3.3 for both CW2D and CWM1 is increased by one to that given in Table 3.2. In both models, a non-reactive tracer that is independent of other components is added. This non-reactive tracer is defined in both liquid and solid phases.

Table 3.3: Definitions of CW2D and CWM1 components in the liquid and solid phases.

| **Component** | **1** | **2** | **3** | **4** | **5** | **6** | **7** | **8** | **9** | **10** | **11** | **12** | **13** | **14** | **15** | **16** | **17** |
|---|---|---|---|---|---|---|---|---|---|---|---|---|---|---|---|---|---|
| **CW2D** | L | L+S | L+S | L+S | S | S | S | L+S | L | L | L | L+S | L+S | - | - | - | - |
| **CWM1** | L | L+S | L+S | L+S | L+S | L | L | L | L+S | L+S | S | S | S | S | S | S | L+S |

L = defined in the liquid phase only; S = defined in the solid phase only; L+S = defined in both liquid and solid phases

Table 3.4 compares the processes defined in the CW2D and CWM1 model formulations. In CW2D only aerobic and anoxic processes are defined. Two main types of bacteria are modeled, heterotrophic and autotrophic bacteria. One special feature of CW2D is that nitrification is modeled as a two-step process, from ammonia over nitrite to nitrate.

Since in CWM1 anaerobic processes are also defined, 6 different types of bacteria needs to be described. Besides heterotrophic and autotrophic bacteria, also fermenting, acetotrophic methanogenic, acetotrophic sulphate reducing and sulphide oxidising bacteria are defined in order to describe mainly anaerobic processes.

Table 3.4: Comparison of CW2D and CWM1 processes.

| **CW2D** (Langergraber and Šimůnek, 2005) | **CWM1** (Langergraber et al., 2009b) |
|---|---|
| ***Heterotrophic bacteria:*** | ***Heterotrophic bacteria:*** |
| 1. ***Hydrolysis****:* conversion of CS into CR. | *1.* ***Hydrolysis***: conversion of XS into SF. |
| 2. ***Aerobic growth of XH on CR*** (mineralization of organic matter). | 2. ***Aerobic growth of XH on SF*** (mineralization of organic matter). |
| 3. ***Anoxic growth of XH on CR*** (denitrification on NO2N). | 3. ***Aerobic growth of XH on SA*** (mineralization of organic matter). |
| 4. ***Anoxic growth of XH on CR*** (denitrification on NO3N). | 4. ***Anoxic growth of XH on SF*** (denitrification). |
| 5. ***Lysis of XH***. | 5. ***Anoxic growth of XH on SA*** (denitrification). |
| | 6. ***Lysis of XH***. |
| | ***Autotrophic bacteria:*** |
| ***Autotrophic bacteria:*** | 7. Aerobic growth of XA on SNH (nitrification). |
| 6. ***Aerobic growth of XANs on SNH*** (ammonium oxidation). | 8. Lysis of XA. |
| | ***Fermenting bacteria:*** |
| 7. ***Lysis of XANs***. | 9. Growth of XFB (fermentation). |
| 8. ***Aerobic growth of XANb on SNH*** (nitrite oxidation). | 10. Lysis of XFB. |
| | ***Acetotrophic methanogenic bacteria:*** |
| 9. ***Lysis of XANb***. | 11. Growth of XAMB: Anaerobic growth of acetotrophic, methanogenic bacteria XAMB on acetate SA. |
| | 12. Lysis of XAMB. |
| | ***Acetotrophic sulphate reducing bacteria:*** |
| | 13. Growth of XASRB: Anaerobic growth of acetotrophic, sulphate reducing bacteria. |
| | 14. Lysis of XASRB. |
| | ***Sulphide oxidizing bacteria:*** |
| | 15. Aerobic growth of XSOB on SH2S: The opposite process to process 13, the oxidation of SH2S to SSO4. |
| | 16. Anoxic growth of XSOB on SH2S: Similar to process 15 but under anoxic conditions. |
| | 17. Lysis of XSOB. |

## 3.4 CW2D biokinetic model

### 3.4.1 Stoichiometric matrix and reaction rates

Table 3.5 and Table 3.6 show stoichiometric coefficients for ammonium nitrogen and inorganic phosphorus, respectively. Table 3.7 shows the stoichiometric matrix of reactions in CW2D, whereas Table 3.8 shows the reaction rates.

Table 3.5: Stoichiometric coefficients for ammonium nitrogen.

| | |
|---|---|
| $\nu_{1,N}$ = | $i_{N,CS}$ - (1- $f_{Hyd,CI}$) . $i_{N,CR}$ - $f_{Hyd,CI}$ . $i_{N,CI}$ |
| $\nu_{2,N}$ = | $1/Y_H$ . $i_{N,CR}$ - $i_{N,BM}$ |
| $\nu_{3,N}$ = | $1/Y_H$ . $i_{N,CR}$ - $i_{N,BM}$ |
| $\nu_{4,N}$ = | $1/Y_H$ . $i_{N,CR}$ - $i_{N,BM}$ |
| $\nu_{5,N}$ = | $i_{N,BM}$ - (1 - $f_{BM,CR}$ - $f_{BM,CI}$) . $i_{N,CS}$ - $f_{BM,CR}$ . $i_{N,CR}$ - $f_{BM,CI}$ . $i_{N,CI}$ |
| $\nu_{6,N}$ = | - $1/Y_{ANs}$ - $i_{N,BM}$ |
| $\nu_{7,N}$ = | $i_{N,BM}$ - (1 - $f_{BM,CR}$ - $f_{BM,CI}$) . $i_{N,CS}$ - $f_{BM,CR}$ . $i_{N,CR}$ - $f_{BM,CI}$ . $i_{N,CI}$ |
| $\nu_{8,N}$ = | - $i_{N,BM}$ |
| $\nu_{9,N}$ = | $i_{N,BM}$ - (1 - $f_{BM,CR}$ - $f_{BM,CI}$) . $i_{N,CS}$ - $f_{BM,CR}$ . $i_{N,CR}$ - $f_{BM,CI}$ . $i_{N,CI}$ |

See Table 3.10 for definitions of the composition and stoichiometric parameters.

Table 3.6: Stoichiometric coefficients for inorganic phosphorus.

| | |
|---|---|
| $\nu_{1,P}$ = | $i_{P,CS}$ - (1- $f_{Hyd,CI}$) . $i_{P,CR}$ - $f_{Hyd,CI}$ . $i_{P,CI}$ |
| $\nu_{2,P}$ = | $1/Y_H$ . $i_{P,CR}$ - $i_{P,BM}$ |
| $\nu_{3,P}$ = | $1/Y_H$ . $i_{P,CR}$ - $i_{P,BM}$ |
| $\nu_{4,P}$ = | $1/Y_H$ . $i_{P,CR}$ - $i_{P,BM}$ |
| $\nu_{5,P}$ = | $i_{P,BM}$ - (1 - $f_{BM,CR}$ - $f_{BM,CI}$) . $i_{P,CS}$ - $f_{BM,CR}$ . $i_{P,CR}$ - $f_{BM,CI}$ . $i_{P,CI}$ |
| $\nu_{6,P}$ = | - $i_{P,BM}$ |
| $\nu_{7,P}$ = | $i_{P,BM}$ - (1 - $f_{BM,CR}$ - $f_{BM,CI}$) . $i_{P,CS}$ - $f_{BM,CR}$ . $i_{P,CR}$ - $f_{BM,CI}$ . $i_{P,CI}$ |
| $\nu_{8,P}$ = | - $i_{P,BM}$ |
| $\nu_{9,P}$ = | $i_{P,BM}$ - (1 - $f_{BM,CR}$ - $f_{BM,CI}$) . $i_{P,CS}$ - $f_{BM,CR}$ . $i_{P,CR}$ - $f_{BM,CI}$ . $i_{P,CI}$ |

See Table 3.10 for definitions of the composition and stoichiometric parameters.

Table 3.7: Stoichiometric matrix of reactions in CW2D (Langergraber and Šimůnek, 2005; see Table 3.10 for definitions of the stoichiometric coefficients).

| R | *N*: Components: | 1 O2 | 2 CR | 3 CS | 4 CI | 5 XH | 6 XANs | 7 XANb | 8 NH4N | 9 NO2N | 10 NO3N | 11 N2N | 12 IP |
|---|---|---|---|---|---|---|---|---|---|---|---|---|---|
| | | gO2 | gCOD | | | | | | gN | | | | gP |
| | | | | Heterotrophic organisms | | | | | | | | | |
| 1 | Hydrolysis | | $1 - f_{Hyd,CR}$ | $-1$ | $f_{Hyd,CI}$ | | | | $\upsilon_{1,N}$ | | | | $\upsilon_{1,P}$ |
| 2 | Aerobic growth of heterotrophs on readily biodegradable COD | $1 - 1/Y_H$ | $-1/Y_H$ | | | 1 | | | $\upsilon_{2,N}$ | | | | $\upsilon_{2,P}$ |
| 3 | Nitrate-based growth of heterotrophs on readily biodegradable COD | | $-1/Y_H$ | | | 1 | | | $\upsilon_{3,N}$ | | $-(1 - Y_H)/2.86Y_H$ | $(1 - Y_H)/2.86Y_H$ | $\upsilon_{3,P}$ |
| 4 | Nitrite-based growth of heterotrophs on readily biodegradable COD | | $-1/Y_H$ | | | 1 | | | $\upsilon_{4,N}$ | $-(1 - Y_H)/1.71Y_H$ | | $(1 - Y_H)/1.71Y_H$ | $\upsilon_{4,P}$ |
| 5 | Lysis of heterotrophs | | $f_{BM,CR}$ | $1 - f_{BM,CR} - f_{BM,CI}$ | $f_{BM,CI}$ | $-1$ | | | $\upsilon_{5,N}$ | | | | $\upsilon_{5,P}$ |
| | | | | Autotrophic organisms 1—*Nitrosomonas* | | | | | | | | | |
| 6 | Aerobic growth of *Nitrosomonas* on ammonium | $-(3.43 - Y_{ANs})/Y_{ANs}$ | | | | | 1 | | $i_{N,BM}$ | $-1/Y_{ANs}$ | $1/Y_{ANs}$ | | $\upsilon_{6,P}$ |
| 7 | Lysis of *Nitrosomonas* | | $f_{BM,CR}$ | $1 - f_{BM,CR} - f_{BM,CI}$ | $f_{BM,CI}$ | | $-1$ | | $\upsilon_{7,N}$ | | | | $\upsilon_{7,P}$ |
| | | | | Autotrophic organisms 2—*Nitrobacter* | | | | | | | | | |
| 8 | Aerobic growth of *Nitrobacter* on nitrite | | | | | | | 1 | $\upsilon_{8,N}$ | $-1/Y_{ANb}$ | $1/Y_{ANb}$ | | $\upsilon_{8,P}$ |
| 9 | Lysis of *Nitrobacter* | $-(1.14 - Y_{ANb})/Y_{ANb}$ | $f_{BM,CR}$ | $1 - f_{BM,CR} - f_{BM,CI}$ | $f_{BM,CI}$ | | | $-1$ | $\upsilon_{9,N}$ | | | | $\upsilon_{9,P}$ |

Table 3.8: Reaction rates in CW2D (Langergraber and Šimůnek, 2005).

| R | Process / Reaction rate $rc_j$ |
|---|---|
| **Heterotrophic organisms** | |
| 1 | Hydrolysis<br>$K_h \cdot \frac{c_{CS}/c_{XH}}{K_X + c_{CS}/c_{XH}} \cdot c_{XH}$ |
| 2 | Aerobic growth of heterotrophs on readily biodegradable COD<br>$\mu_H \cdot \frac{c_{O2}}{K_{Het,O2} + c_{O2}} \cdot \frac{c_{CR}}{K_{Het,CR} + c_{CR}} \cdot f_{N,Het} \cdot c_{XH}$ |
| 3 | NO3-growth of heterotrophs on readily biodegradable COD<br>$\mu_{DN} \cdot \frac{K_{DN,O2}}{K_{DN,O2} + c_{O2}} \cdot \frac{c_{NO3}}{K_{DN,NO3} + c_{NO3}} \cdot \frac{K_{DN,NO2}}{K_{DN,NO2} + c_{NO2}} \cdot \frac{c_{CR}}{K_{DN,CR} + c_{CR}} \cdot f_{N,DN} \cdot c_{XH}$ |
| 4 | NO2-growth of heterotrophs on readily biodegradable COD<br>$\mu_{DN} \cdot \frac{K_{DN,O2}}{K_{DN,O2} + c_{O2}} \cdot \frac{c_{NO2}}{K_{DN,NO2} + c_{NO2}} \cdot \frac{c_{CR}}{K_{DN,CR} + c_{CR}} \cdot f_{N,DN} \cdot c_{XH}$ |
| 5 | Lysis of heterotrophs<br>$b_H \cdot c_{XH}$ |
| **Autotrophic organisms 1 – *Nitrosomonas*** | |
| 6 | Aerobic growth of *Nitrosomonas* on NH4<br>$\mu_{ANs} \cdot \frac{c_{O2}}{K_{ANs,O2} + c_{O2}} \cdot \frac{c_{NH4}}{K_{ANs,NH4} + c_{NH4}} \cdot \frac{c_{IP}}{K_{ANs,IP} + c_{IP}} \cdot c_{XANs}$ |
| 7 | Lysis of *Nitrosomonas*<br>$b_{HANs} \cdot c_{XANs}$ |
| **Autotrophic organisms 2 – *Nitrobacter*** | |
| 8 | Aerobic growth of *Nitrobacter* on NO2<br>$\mu_{ANb} \cdot \frac{c_{O2}}{K_{ANb,O2} + c_{O2}} \cdot \frac{c_{NO2}}{K_{ANb,NO2} + c_{NO2}} \cdot f_{N,ANb} \cdot c_{XANb}$ |
| 9 | Lysis of *Nitrobacter*<br>$b_{HANb} \cdot c_{XANb}$ |
| **Conversion of solid and liquid phase concentrations** | |
| | $c_{XY} = \frac{\rho}{\theta} \cdot s_{XY}$ , where $Y = H, ANs, ANb$ |
| **Factor for nutrients** | |
| | $f_{N,x} = \frac{c_{NH4}}{K_{x,NH4} + c_{NH4}} \cdot \frac{c_{IP}}{K_{x,IP} + c_{IP}}$ , where $x = Het, DN, ANb$ |

See Table 3.9 for definitions of rate coefficients.

### 3.4.2 Model parameters

Table 3.9 shows the kinetic parameters, and Table 3.10 the temperature dependences, stoichiometric parameters, composition parameters and parameters describing oxygen transfer for the CW2D biokinetic model as described in Langergraber and Šimůnek (2005).

Table 3.9: Kinetic parameters in the CW2D biokinetic model (Langergraber and Šimůnek, 2005).

| | Description [unit] | Value |
|---|---|---|
| **Hydrolysis** | | for 20°C (10°C) |
| $K_h$ | hydrolysis rate constant [1/d] | 3 (2) |
| $K_X$ | saturation/inhibition coefficient for hydrolysis [g $COD_{CS}$/g $COD_{BM}$] | 0.1 (0.22) * |
| **Heterotrophic bacteria (aerobic growth)** | | |
| $\mu_H$ | maximum aerobic growth rate on CR [1/d] | 6 (3) |
| $b_H$ | rate constant for lysis [1/d] | 0.4 (0.2) |
| $K_{het,O2}$ | saturation/inhibition coefficient for $S_O$ [mg $O_2$/L] | 0.2 |
| $K_{het,CR}$ | saturation/inhibition coefficient for substrate [mg $COD_{CR}$/L] | 2 |
| $K_{het,NH4N}$ | saturation/inhibition coefficient for NH4 (nutrient) [mg N/L] | 0.05 |
| $K_{het,IP}$ | saturation/inhibition coefficient for P [mg N/L] | 0.01 |
| **Heterotrophic bacteria (denitrification)** | | |
| $\mu_{DN}$ | maximum aerobic growth rate on CR [1/d] | 4.8 (2.4) |
| $K_{DN,O2}$ | saturation/inhibition coefficient for $S_O$ [mg $O_2$/L] | 0.2 |
| $K_{DN,NO3N}$ | saturation/inhibition coefficient for NO3 [mg N/L] | 0.5 |
| $K_{DN,NO2N}$ | saturation/inhibition coefficient for NO2 [mg N/L] | 0.5 |
| $K_{DN,CR}$ | saturation/inhibition coefficient for substrate [mg $COD_{CR}$/L] | 4 |
| $K_{DN,NH4N}$ | saturation/inhibition coefficient for NH4 (nutrient) [mg N/L] | 0.05 |
| $K_{DN,IP}$ | saturation/inhibition coefficient for P [mg N/L] | 0.01 |
| **Ammonia oxidising bacteria (*Nitrosomonas* spp.)** | | |
| $\mu_{ANs}$ | maximum aerobic growth rate on $S_{NH}$ [1/d] | 0.9 (0.3) |
| $b_{ANs}$ | rate constant for lysis [1/d] | 0.15 (0.05) |
| $K_{ANs,O2}$ | saturation/inhibition coefficient for $S_O$ [mg $O_2$/L] | 1 |
| $K_{ANs,NH4N}$ | saturation/inhibition coefficient for NH4 [mg N/L] | 0.5 |
| $K_{ANs,IP}$ | saturation/inhibition coefficient for P [mg N/L] | 0.01 |
| **Nitrite oxidising bacteria (*Nitrobacter* spp.)** | | |
| $\mu_{ANb}$ | maximum aerobic growth rate on $S_{NH}$ [1/d] | 1 (0.35) |
| $b_{ANb}$ | rate constant for lysis [1/d] | 0.15 (0.05) * |
| $K_{ANb,O2}$ | saturation/inhibition coefficient for $S_O$ [mg $O_2$/L] | 0.1 |
| $K_{ANb,NO2N}$ | saturation/inhibition coefficient for NO2 [mg N/L] | 0.1 |
| $K_{ANb,NH4N}$ | saturation/inhibition coefficient for NH4 (nutrient) [mg N/L] | 0.05 |
| $K_{ANb,IP}$ | saturation/inhibition coefficient for P [mg N/L] | 0.01 |

* Langergraber (2007)

Table 3.10: Temperature dependences, stoichiometric parameters, composition parameters and parameters describing oxygen transfer in the CW2D biokinetic model (Langergraber and Šimůnek, 2005).

| **Parameter** | **Description [unit]** | **Value** |
|---|---|---|
| **Temperature dependences (**activation energy [J/mol] for Arrhenius equation**)** | | |
| Tdep_het | Activation energy for processes caused by XH [J/mol] | 47800 |
| Tdep_aut | Activation energy for processes caused by XA [J/mol] | 69000 |
| Tdep_Kh | Activation energy Hydrolyses [J/mol] | 28000 |
| Tdep_KX | Activation energy factor KX for hydrolyses [J/mol] | -53000 * |
| Tdep_KNHA | Activation energy for factor KNHA for nitrification [J/mol] | -160000 * |
| **Stoichiometric parameters** | | |
| $f_{\mathrm{Hyd,CI}}$ | production of CI in hydrolysis | 0.0 |
| $f_{\mathrm{BM,CR}}$ | fraction of CR generated in biomass lysis | 0.1 |
| $f_{\mathrm{BM,CI}}$ | fraction of CI generated in biomass lysis | 0.02 |
| $Y_{\mathrm{Het}}$ | yield coefficient for XH | 0.63 |
| $Y_{\mathrm{ANs}}$ | yield coefficient for XANs | 0.24 |
| $Y_{\mathrm{ANb}}$ | yield coefficient for XANb | 0.24 |
| **Composition parameters** | | |
| $i_{\mathrm{N,CR}}$ | N content of CR [g N/g $COD_{CR}$] | 0.03 |
| $i_{\mathrm{N,CS}}$ | N content of CS [g N/g $COD_{CS}$] | 0.04 |
| $i_{\mathrm{N,CI}}$ | N content of CI [g N/g $COD_{CI}$] | 0.01 |
| $i_{\mathrm{N,BM}}$ | N content of biomass [g N/g $COD_{BM}$] | 0.07 |
| $i_{\mathrm{P,CR}}$ | P content of CR [g P/g $COD_{CR}$] | 0.01 |
| $i_{\mathrm{P,CS}}$ | P content of CS [g P/g $COD_{CS}$] | 0.01 |
| $i_{\mathrm{P,CI}}$ | P content of CI [g P/g $COD_{CI}$] | 0.01 |
| $i_{\mathrm{P,BM}}$ | P content of biomass [g P/g $COD_{BM}$] | 0.02 |
| **Oxygen** | | |
| cO2_sat_20 | saturation concentration of oxygen [g/m³] | 9.18 |
| Tdep_cO2_sat | activation energy for saturation concentration of oxygen [J/mol] | -15000 |
| rate_O2 | re-aeration rate [1/d] | 240 |

* Langergraber (2007)

## 3.5 CWM1 biokinetic model

### 3.5.1 Stoichiometric matrix and reaction rates

Table 3.11 shows the stoichiometric matrix of reactions in CWM1, Table 3.12 stoichiometric coefficients for ammonium nitrogen, and Table 3.13 and Table 3.14 the reaction rates.

Table 3.11: Stoichiometric matrix of reactions in CWM1 (Langergraber et al., 2009b; see Table 3.16 for definitions of the stoichiometric coefficients).

| j ↓ | i → Process component expressed as → | 1 $S_O$ $O_2$ | 2 $S_F$ COD | 3 $S_A$ COD | 4 $S_I$ COD | 5 $S_{NH}$ N | 6 $S_{NO}$ N | 7 $S_{SO4}$ S | 8 $S_{H2S}$ S | 9 $X_S$ COD | 10 $X_I$ COD | 11 $X_H$ COD | 12 $X_A$ COD | 13 $X_{FB}$ COD | 14 $X_{AMB}$ COD | 15 $X_{ASRB}$ COD | 16 $X_{SOB}$ COD |
|---|---|---|---|---|---|---|---|---|---|---|---|---|---|---|---|---|---|
| 1 | Hydrolysis | | $1-f_{Hyd,SI}$ | | $f_{Hyd,SI}$ | $v_{5,1}$ | | | | $-1$ | | | | | | | |
| 2 | Aerobic growth of $X_H$ on $S_F$ | $1-\frac{1}{Y_H}$ | $-1/Y_H$ | | | $v_{5,2}$ | | | | | | 1 | | | | | |
| 3 | Anoxic growth of $X_H$ on $S_F$ | | $-1/Y_H$ | | | $v_{5,3}$ | $-\frac{1-Y_H}{2.86\,Y_H}$ | | | | | 1 | | | | | |
| 4 | Aerobic growth of $X_H$ on $S_A$ | $1-\frac{1}{Y_H}$ | | $-1/Y_H$ | | $v_{5,4}$ | | | | | | 1 | | | | | |
| 5 | Anoxic growth of $X_H$ on $S_A$ | | | $-1/Y_H$ | | $v_{5,5}$ | $-\frac{1-Y_H}{2.86\,Y_H}$ | | | | | 1 | | | | | |
| 6 | Lysis of $X_H$ | | $f_{BM,SF}$ | | | $v_{5,6}$ | | | | $v_{9,Lysis}$ | $f_{BM,XI}$ | $-1$ | | | | | |
| 7 | Aerobic growth of $X_A$ on $S_{NH}$ | $-\frac{4.57-Y_A}{Y_A}$ | | | | $-i_{N,BM}-\frac{1}{Y_A}$ | $1/Y_A$ | | | | | | 1 | | | | |
| 8 | Lysis of $X_A$ | | $f_{BM,SF}$ | | | $v_{5,8}$ | | | | $v_{9,Lysis}$ | $f_{BM,XI}$ | | $-1$ | | | | |
| 9 | Growth of $X_{FB}$ | | $-1/Y_{FB}$ | $\frac{1-Y_{FB}}{Y_{FB}}$ | | $v_{5,9}$ | | | | | | | | 1 | | | |
| 10 | Lysis of $X_{FB}$ | | $f_{BM,SF}$ | | | $v_{5,10}$ | | | | $v_{9,Lysis}$ | $f_{BM,XI}$ | | | $-1$ | | | |
| 11 | Growth of $X_{AMB}$ | | | $-1/Y_{AMB}$ | | $v_{5,11}$ | | | | | | | | | 1 | | |
| 12 | Lysis of $X_{AMB}$ | | $f_{BM,SF}$ | | | $v_{5,12}$ | | | | $v_{9,Lysis}$ | $f_{BM,XI}$ | | | | $-1$ | | |
| 13 | Growth of $X_{ASRB}$ | | | $-1/Y_{ASRB}$ | | $v_{5,13}$ | | $-\frac{1-Y_{ASRB}}{2\cdot Y_{ASRB}}$ | $\frac{1-Y_{ASRB}}{2\cdot Y_{ASRB}}$ | | | | | | | 1 | |
| 14 | Lysis of $X_{ASRB}$ | | $f_{BM,SF}$ | | | $v_{5,14}$ | | | | $v_{9,Lysis}$ | $f_{BM,XI}$ | | | | | $-1$ | |
| 15 | Aerobic growth of $X_{SOB}$ on $S_{H2S}$ | $-\frac{2-Y_{SOB}}{Y_{SOB}}$ | | | | $v_{5,15}$ | | $1/Y_{SOB}$ | $-1/Y_{SOB}$ | | | | | | | | 1 |
| 16 | Anoxic growth of $X_{SOB}$ on $S_{H2S}$ | | | | | $v_{5,16}$ | $-\frac{1-Y_{SOB}}{0.875\cdot Y_{SOB}}$ | $1/Y_{SOB}$ | $-1/Y_{SOB}$ | | | | | | | | 1 |
| 17 | Lysis of $X_{SOB}$ | | $f_{BM,SF}$ | | | $v_{5,17}$ | | | | $v_{9,Lysis}$ | $f_{BM,XI}$ | | | | | | $-1$ |

$v_{9,Lysis} = 1 - f_{BM,SF} - f_{BM,XI}$

Table 3.12: Stoichiometric coefficients for ammonia nitrogen.

| | |
|---|---|
| $\nu_{5,1} =$ | $i_{N,XS} - (1\text{-}f_{HYD,SI}) * i_{N,SF} - f_{HYD,SI} * i_{N,SI}$ |
| $\nu_{5,2} = \nu_{5,3} =$ | $i_{N,SF}/Y_H - i_{N,BM}$ |
| $\nu_{5,4} = \nu_{5,5} = \nu_{5,11} = \nu_{5,13} = \nu_{5,15} = \nu_{5,16} =$ | $- i_{N,BM}$ |
| $\nu_{5,6} = \nu_{5,8} = \nu_{5,10} = \nu_{5,12} = \nu_{5,14} = \nu_{5,17} =$ | $i_{N,BM} - f_{BM,SF} * i_{N,SF} - (1 - f_{BM,SF} - f_{BM,XI}) * i_{N,XS} - f_{BM,XI} * i_{N,XI}$ |
| $\nu_{5,7} =$ | $- i_{N,BM} - \frac{1}{Y_A}$ |
| $\nu_{5,9} =$ | $i_{N,SF}/Y_{FB} - i_{N,BM}$ |

See Table 3.16 for definitions of the composition and stoichiometric parameters.

Table 3.13: Reaction rates in CWM1 - part 1 (Langergraber et al., 2009b).

| R | Process / Reaction rate $rc_j$ |
|---|---|
| **Heterotrophic organisms** | |
| 1 | Hydrolysis<br>$k_h * \left[\frac{X_S/(X_H + X_{FB})}{K_X + (X_S/(X_H + X_{FB}))}\right] * (X_H + \eta_h * X_{FB})$ |
| 2 | Aerobic growth of XH on SF (mineralization)<br>$\mu_H * \left(\frac{S_F}{K_{SF} + S_F}\right) * \left(\frac{S_F}{S_F + S_A}\right) * \left(\frac{S_O}{K_{OH} + S_o}\right) * \left(\frac{S_{NH}}{K_{NHH} + S_{NH}}\right) * \left(\frac{K_{H2SH}}{K_{H2SH} + S_{H2S*}}\right) * X_H$ |
| 3 | Aerobic growth of XH on SA (mineralization)<br>$\eta_g * \mu_H * \left(\frac{S_F}{K_{SF} + S_F}\right) * \left(\frac{S_F}{S_F + S_A}\right) * \left(\frac{K_{OH}}{K_{OH} + S_o}\right) * \left(\frac{S_{NO}}{K_{NOH} + S_{NO}}\right) * \left(\frac{S_{NH}}{K_{NHH} + S_{NH}}\right) * \left(\frac{K_{H2SH}}{K_{H2SH} + S_{H2S*}}\right) * X_H$ |
| 4 | Anoxic growth of XH on SF (denitrification)<br>$\mu_H * \left(\frac{S_A}{K_{SA} + S_A}\right) * \left(\frac{S_A}{S_F + S_A}\right) * \left(\frac{S_O}{K_{OH} + S_o}\right) * \left(\frac{S_{NH}}{K_{NHH} + S_{NH}}\right) * \left(\frac{K_{H2SH}}{K_{H2SH} + S_{H2S*}}\right) * X_H$ |
| 5 | Anoxic growth of XH on SA (denitrification)<br>$\eta_g * \mu_H * \left(\frac{S_A}{K_{SA} + S_A}\right) * \left(\frac{S_A}{S_F + S_A}\right) * \left(\frac{K_{OH}}{K_{OH} + S_o}\right) * \left(\frac{S_{NO}}{K_{NOH} + S_{NO}}\right) * \left(\frac{S_{NH}}{K_{NHH} + S_{NH}}\right) * \left(\frac{K_{H2SH}}{K_{H2SH} + S_{H2S*}}\right) * X_H$ |
| 6 | Lysis of XH<br>$b_H * X_H$ |
| **Autotrophic bacteria** | |
| 7 | Aerobic growth of XA on SNH (nitrification)<br>$\mu_A * \left(\frac{S_{NH}}{K_{NHA} + S_{NH}}\right) * \left(\frac{S_O}{K_{OA} + S_o}\right) * \left(\frac{K_{H2SA}}{K_{H2SA} + S_{H2S*}}\right) * X_A$ |
| 8 | Lysis of XA<br>$b_A * X_A$ |
| **Fermenting bacteria** | |
| 9 | Growth of XFB (fermentation)<br>$\mu_{FB} * \left(\frac{S_F}{K_{SFB} + S_F}\right) * \left(\frac{K_{H2SFB}}{K_{H2SFB} + S_{H2S*}}\right) * \left(\frac{K_{OFB}}{K_{OFB} + S_O}\right) * \left(\frac{K_{NOFB}}{K_{NOFB} + S_{NO}}\right) * \left(\frac{S_{NH}}{K_{NHFB} + S_{NH}}\right) * X_{FB}$ |
| 10 | Lysis of XFB<br>$b_{FB} * X_{FB}$ |

See Table 3.15 for definitions of rate coefficients.

Table 3.14: Reaction rates in CWM1 - part 2 (Langergraber et al., 2009b).

| | |
|---|---|
| **Acetotrophic methanogenic bacteria** | |
| 11 | Growth of XAMB<br>$\mu_{AMB} * \left(\frac{S_A}{K_{SAMB}+S_A}\right) * \left(\frac{K_{H2SAMB}}{K_{H2SAMB}+S_{H2S*}}\right) * \left(\frac{K_{OAMB}}{K_{OAMB}+S_O}\right) * \left(\frac{K_{NOAMB}}{K_{NOAMB}+S_{NO}}\right) * \left(\frac{S_{NH}}{K_{NHAMB}+S_{NH}}\right) * X_{AMB}$ |
| 12 | Lysis of XAMB<br>$b_{AMB} * X_{AMB}$ |
| **Acetotrophic sulphate reducing bacteria** | |
| 13 | Growth of XASRB<br>$\mu_{ASRB} * \left(\frac{S_A}{K_{SASRB}+S_A}\right) * \left(\frac{S_{SO4}}{K_{SOASRB}+S_{SO4}}\right) * \left(\frac{K_{H2SASRB}}{K_{H2SASRB}+S_{H2S*}}\right) * \left(\frac{K_{OASRB}}{K_{OASRB}+S_O}\right) * \left(\frac{K_{NOASRB}}{K_{NOASRB}+S_{NO}}\right) * \left(\frac{S_{NH}}{K_{NHASRB}+S_{NH}}\right) * X_{ASRB}$ |
| 14 | Lysis of XASRB<br>$b_{ASRB} * X_{ASRB}$ |
| **Sulphide oxidizing bacteria** | |
| 15 | Aerobic growth of XSOB on SH2S<br>$\mu_{SOB} * \left(\frac{S_{H2S}}{K_{SSOB}+S_{H2S}}\right) * \left(\frac{S_O}{K_{OSOB}+S_O}\right) * \left(\frac{S_{NH}}{K_{NHSOB}+S_{NH}}\right) * X_{SOB}$ |
| 16 | Anoxic growth of XSOB on SH2S<br>$\mu_{SOB} * \eta_{SOB} * \left(\frac{S_{H2S}}{K_{SSOB}+S_{H2S}}\right) * \left(\frac{S_{NO}}{K_{NOSOB}+S_{NO}}\right) * \left(\frac{K_{OSOB}}{K_{OSOB}+S_O}\right) * \left(\frac{S_{NH}}{K_{NHSOB}+S_{NH}}\right) * X_{SOB}$ |
| 17 | Lysis of XSOB<br>$b_{SOB} * X_{SOB}$ |

See Table 3.15 for definitions of rate coefficients.

### 3.5.2 Model parameters

Table 3.15 shows the kinetic parameters in the CWM1 biokinetic model as described in Langergraber et al. (2009b).

Table 3.15: Kinetic parameters in the CWM1 biokinetic model (Langergraber et al., 2009b).

| Parameter | Description [unit] | Value |
|---|---|---|
| **Hydrolysis** | | for 20°C (10°C) |
| $K_h$ | hydrolysis rate constant [1/d] | 3 (2) |
| $K_X$ | saturation/inhibition coefficient for hydrolysis [g $COD_{SF}$/g $COD_{BM}$] | 0.1 (0.22) |
| $\eta_H$ | correction factor for hydrolysis by fermenting bacteria [-] | 0.1 |
| **Heterotrophic bacteria (aerobic growth and denitrification)** | | |
| $\mu_H$ | maximum aerobic growth rate on $S_F$ and $S_A$ [1/d] | 6 (3) |
| $\eta_g$ | correction factor for denitrification by XH [-] | 0.8 |
| $b_H$ | rate constant for lysis [1/d] | 0.4 (0.2) |
| $K_{OH}$ | saturation/inhibition coefficient for $S_O$ [mg $O_2$/L] | 0.2 |
| $K_{SF}$ | saturation/inhibition coefficient for $S_F$ [mg $COD_{SF}$/L] | 2 |
| $K_{SA}$ | saturation/inhibition coefficient for $S_A$ [mg $COD_{SA}$/L] | 4 |
| $K_{NOH}$ | saturation/inhibition coefficient for $S_{NO}$ [mg N/L] | 0.5 |
| $K_{NHH}$ | saturation/inhibition coefficient for $S_{NH}$ (nutrient) [mg N/L] | 0.05 |
| $K_{H2SH}$ | saturation/inhibition coefficient for $S_{H2S}$ [mg S/L] | 140 |
| **Autotrophic bacteria** | | |
| $\mu_A$ | maximum aerobic growth rate on $S_{NH}$ [1/d] | 1 (0.35) |
| $b_A$ | rate constant for lysis [1/d] | 0.15 (0.05) |
| $K_{OA}$ | saturation/inhibition coefficient for $S_O$ [mg $O_2$/L] | 1 |
| $K_{NHA}$ | saturation/inhibition coefficient for $S_{NH}$ [mg N/L] | 0.5 (5) |
| $K_{H2SA}$ | saturation/inhibition coefficient for $S_{H2S}$ [mg S/L] | 140 |
| **Fermenting bacteria** | | |
| $\mu_{FB}$ | maximum aerobic growth rate for $X_{FB}$ [1/d] | 3 (1.5) |
| $b_{FB}$ | rate constant for lysis [1/d] | 0.02 |
| $K_{OFB}$ | saturation/inhibition coefficient for $S_O$ [mg $O_2$/L] | 0.2 |
| $K_{SFB}$ | saturation/inhibition coefficient for $S_F$ [mg $COD_{SF}$/L] | 28 |
| $K_{NOFB}$ | saturation/inhibition coefficient for $S_{NO}$ [mg N/L] | 0.5 |
| $K_{NHFB}$ | saturation/inhibition coefficient for $S_{NH}$ (nutrient) [mg N/L] | 0.01 |
| $K_{H2SFB}$ | saturation/inhibition coefficient for $S_{H2S}$ [mg S/L] | 140 |
| **Acetotrophic methanogenic bacteria** | | |
| $\mu_{AMB}$ | maximum aerobic growth rate on for $X_{AMB}$ [1/d] | 0.085 |
| $b_{AMB}$ | rate constant for lysis [1/d] | 0.008 |
| $K_{OAMB}$ | saturation/inhibition coefficient for $S_O$ [mg $O_2$/L] | 0.0002 |
| $K_{SAMB}$ | saturation/inhibition coefficient for $S_A$ [mg $COD_{SA}$/L] | 56 |
| $K_{NOAMB}$ | saturation/inhibition coefficient for $S_{NO}$ [mg N/L] | 0.0005 |
| $K_{NHAMB}$ | saturation/inhibition coefficient for $S_{NH}$ (nutrient) [mg N/L] | 0.01 |
| $K_{H2SAMB}$ | saturation/inhibition coefficient for $S_{H2S}$ [mg S/L] | 140 |
| **Acetotrophic sulphate reducing bacteria** | | |
| $\mu_{ASRB}$ | maximum aerobic growth rate for $X_{ASRB}$ [1/d] | 0.18 |
| $b_{ASRB}$ | rate constant for lysis [1/d] | 0.012 |
| $K_{OASRB}$ | saturation/inhibition coefficient for $S_O$ [mg $O_2$/L] | 0.0002 |
| $K_{SASRB}$ | saturation/inhibition coefficient for $S_A$ [mg $COD_{SA}$/L] | 24 |
| $K_{NOASRB}$ | saturation/inhibition coefficient for $S_{NO}$ [mg N/L] | 0.0005 |
| $K_{NHASRB}$ | saturation/inhibition coefficient for $S_{NH}$ (nutrient) [mg N/L] | 0.01 |
| $K_{SOASRB}$ | saturation/inhibition coefficient for $S_{SO4}$ [mg S/L] | 19 |
| $K_{H2SASRB}$ | saturation/inhibition coefficient for $S_{H2S}$ [mg S/L] | 140 |
| **Sulphide oxidizing bacteria** | | |
| $\mu_{SOB}$ | maximum aerobic growth rate for $X_{SOB}$ [1/d] | 5.28 |
| $\eta_{SOB}$ * | correction factor for anoxic growth of $X_{SOB}$ [-] | 0.8 |
| $b_{SOB}$ | rate constant for lysis [1/d] | 0.15 |
| $K_{OSOB}$ | saturation/inhibition coefficient for $S_O$ [mg $O_2$/L] | 0.2 |
| $K_{NOSOB}$ | saturation/inhibition coefficient for $S_{NO}$ [mg N/L] | 0.5 |
| $K_{NHSOB}$ | saturation/inhibition coefficient for $S_{NH}$ (nutrient) [mg N/L] | 0.05 |
| $K_{SSOB}$ | saturation/inhibition coefficient for $S_{H2S}$ [mg S/L] | 0.24 |

* typing error in the original CWM1 publication.

Table 3.16 shows temperature dependences, stoichiometric parameters, composition parameters and parameters describing oxygen transfer as described in Langergraber et al. (2009b).

Table 3.16: Temperature dependences, stoichiometric parameters, composition parameters and parameters describing oxygen transfer in the CW2D biokinetic model (Langergraber et al., 2009b).

| Parameter | Description [unit] | Value |
|---|---|---|
| **Temperature dependences (**activation energy [J/mol] for Arrhenius equation**)** | | |
| Tdep_HyKh | Activation energy Hydrolyses [J/mol] | 28000 |
| Tdep_HyKX | Activation energy factor KX for hydrolyses [J/mol] | -54400 |
| Tdep_H | Activation energy for processes caused by XH [J/mol] | 47800 |
| Tdep_A | Activation energy for processes caused by XA [J/mol] | 75800 |
| Tdep_KNHA | Activation energy for factor KNHA for nitrification [J/mol] | -160000 |
| Tdep_mueFB | Activation energy for XFB growth [J/mol] | 47800 |
| Tdep_bFB | Activation energy for XFB lysis [J/mol] | 0 |
| Tdep_AMB | Activation energy for processes caused by XAMB [J/mol] | 0 |
| Tdep_ASRB | Activation energy for processes caused by XASRB [J/mol] | 0 |
| Tdep_SOB | Activation energy for processes caused by XSOB [J/mol] | 0 |
| **Stoichiometric parameters** | | |
| $f_{Hyd,SI}$ | production of $S_I$ in hydrolysis | 0.0 |
| $f_{BM,SF}$ | fraction of $S_F$ generated in biomass lysis | 0.05 |
| $f_{BM,XI}$ | fraction of $X_I$ generated in biomass lysis | 0.1 |
| $Y_H$ | yield coefficient for XH | 0.63 |
| $Y_A$ | yield coefficient for XA | 0.24 |
| $Y_{FB}$ | yield coefficient for XFB | 0.053 |
| $Y_{AMB}$ | yield coefficient for XAMB | 0.032 |
| $Y_{ASRB}$ | yield coefficient for XASRB | 0.05 |
| $Y_{SOB}$ | yield coefficient for XSOB | 0.12 |
| **Composition parameters** | | |
| $i_{N,SF}$ | N content of $S_F$ [g N/g $COD_{SF}$] | 0.03 |
| $i_{N,SI}$ | N content of $S_I$ [g N/g $COD_{SI}$] | 0.01 |
| $i_{N,XS}$ | N content of $X_S$ [g N/g $COD_{XS}$] | 0.04 |
| $i_{N,XI}$ | N content of $X_I$ [g N/g $COD_{XI}$] | 0.03 |
| $i_{N,BM}$ | N content of biomass [g N/g $COD_{BM}$] | 0.07 |
| **Oxygen** | | |
| cO2_sat_20 | saturation concentration of oxygen [g/m³] | 9.18 |
| Tdep_cO2_sat | activation energy for saturation concentration of oxygen [J/mol] | -15000 |
| rate_O2 | re-aeration rate [1/d] | 240 |

## 3.6 When to use which biokinetic model?

Table 3.17 provides hints which biokinetic model (i.e., CW2D or CWM1) to use for different types of CWs and for what type of processes.

Table 3.17: Application of the biokinetic models for different applications

| **Biokinetic model** | **CW2D**<br>(Langergraber and Šimůnek, 2005) | **CWM1**<br>(Langergraber et al., 2009b) |
|---|---|---|
| **Type of CW** | • VF CWs<br>• Low loaded HF beds | • VF and HF CWs |
| **Processes** | • Modeling P retention in CWs<br>• Modeling nitrification as a 2-step process | • Modeling anaerobic processes<br>• Modeling transport and fate of sulphur |

# 4 Version 2 of HYDRUS GUI

## 4.1 Preliminary remarks

As described already in Langergraber and Šimůnek (2006), concentrations units in the liquid and solid phases, as well as units of the bulk density, are fixed after choosing the length unit. In version 2 of HYDRUS this is done in the "Domain types and Units" window (Figure 4.1). The resulting concentration units are shown in Table 4.1.

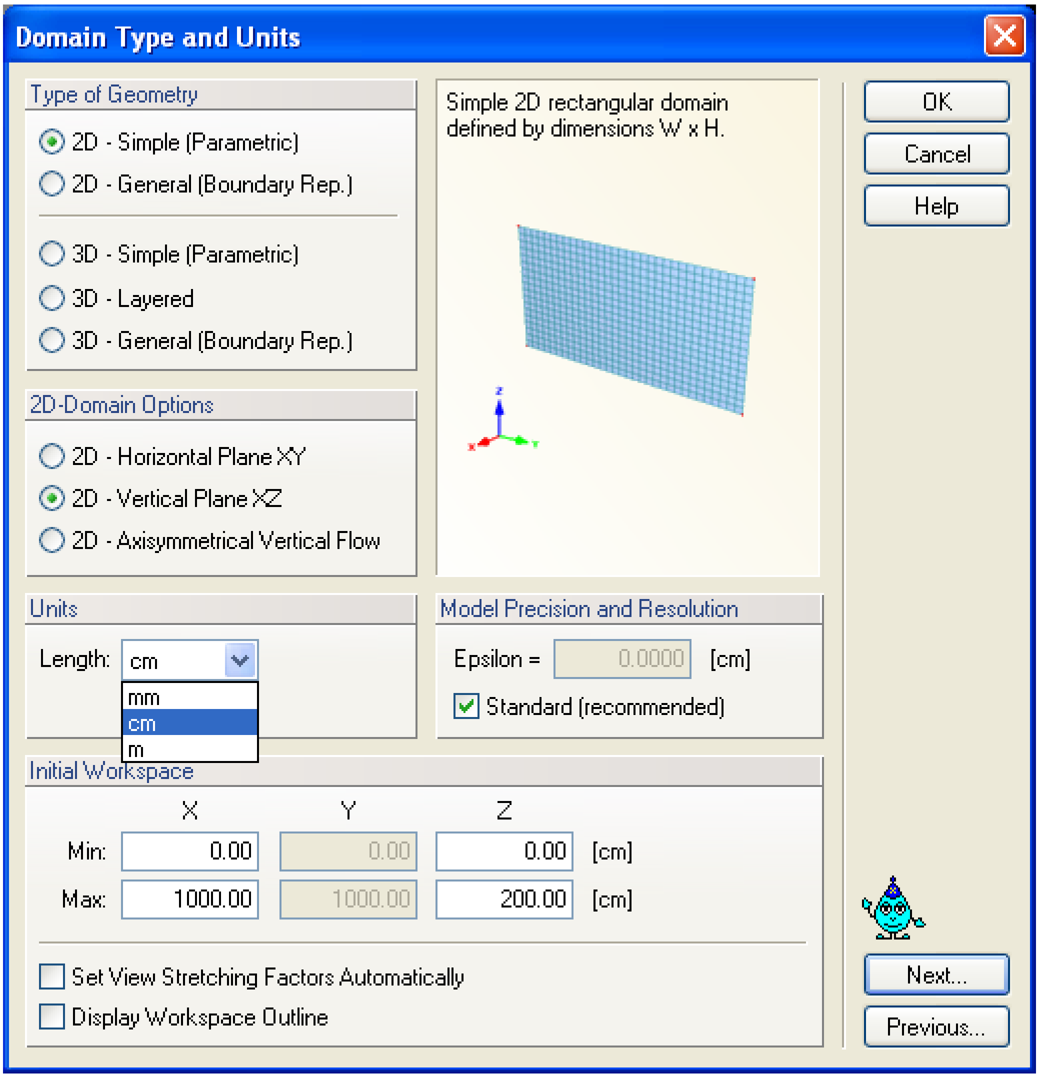


Figure 4.1: The "Domain types and Units" window.

Table 4.1: Units of concentrations in the liquid and solid phases and of the bulk density,

| **Length Units** | **m** | **cm** | **mm** |
|---|---|---|---|
| Concentrations in the liquid phase | g.m$^{-3}$ | µg.cm$^{-3}$ = µg.mL$^{-1}$ | ng.mm$^{-3}$ = ng.µL$^{-1}$ |
| Concentrations in the solid phase | g.t$^{-1}$ | µg.g$^{-1}$ | ng.mg$^{-1}$ |
| Bulk density | t.m$^{-3}$ | g.cm$^{-3}$ | mg.mm$^{-3}$ |

The HYDRUS user interface does not provide conversion of mass units and thus the default values of CW2D and CWM1 must be interpreted based on Table 4.1. Therefore units of concentrations in the liquid and solid phases and of the bulk density are fixed according to Table 4.1 once the length units are chosen.

## 4.2 Pre-processing

### 4.2.1 The "Solute Transport" window

To activate the HYDRUS wetland module in the GUI in the "Solute Transport" window (Figure 4.2), the "***Wetland Module***" box has to be checked. The *Mass Units* have to be set according to the chosen length units (Table 4.1). If the CW2D biokinetic model is chosen in Figure 4.2, the *Number of Solutes* is equal to 13 (12 CW2D components and one non-reactive tracer, independent of the other 12 compounds). If CWM1 is selected (Figure 4.3) the *Number of Solutes* is set to 17 (16 CWM1 components and one non-reactive tracer). If the *Wetland Module* is chosen, the "*Attachment/Detachment Concept*" (used in the standard HYDRUS to simulate the transport of particles, such as colloids, viruses, and bacteria) cannot be used and the *Initial Conditions* cannot be given in *Total Concentrations*. *Initial Conditions* need to be given in liquid or solid phase concentrations.

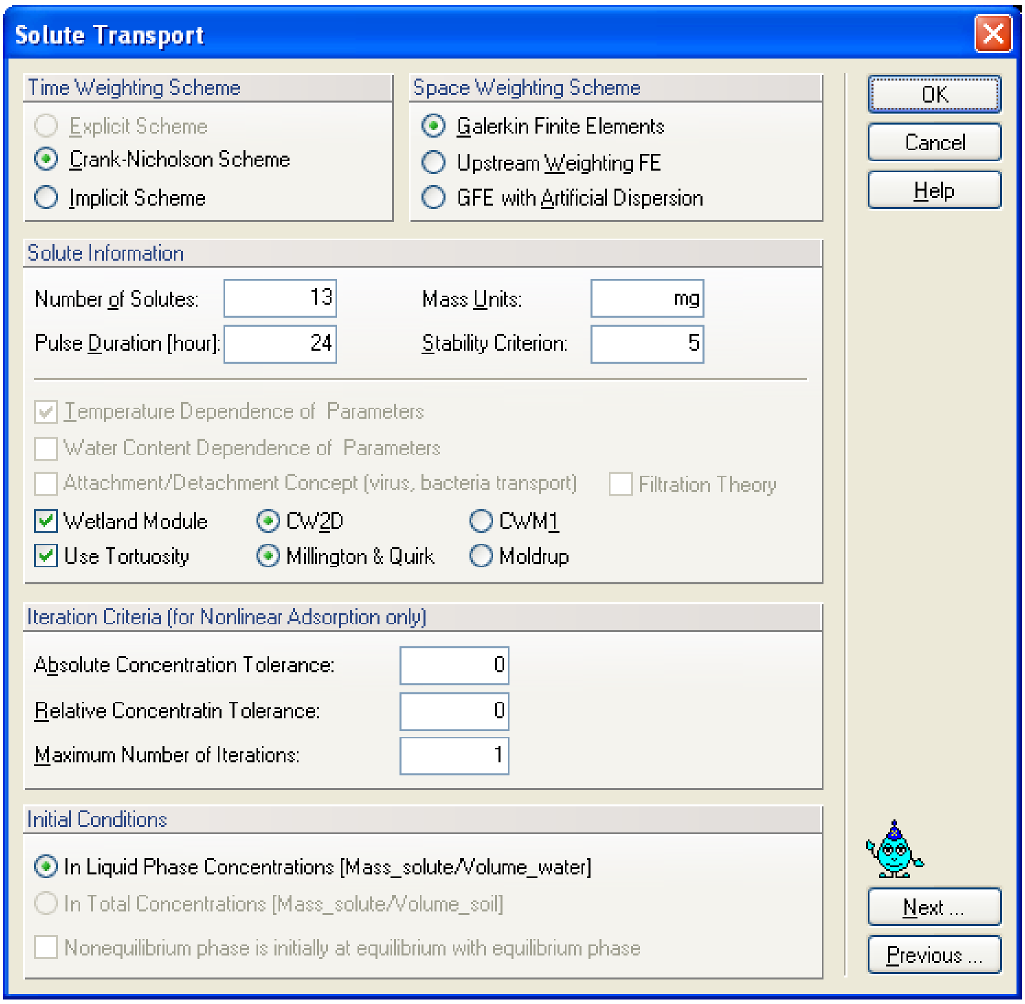


Figure 4.2: The "Solute Transport" window with a selection of the CW2D biokinetic model.

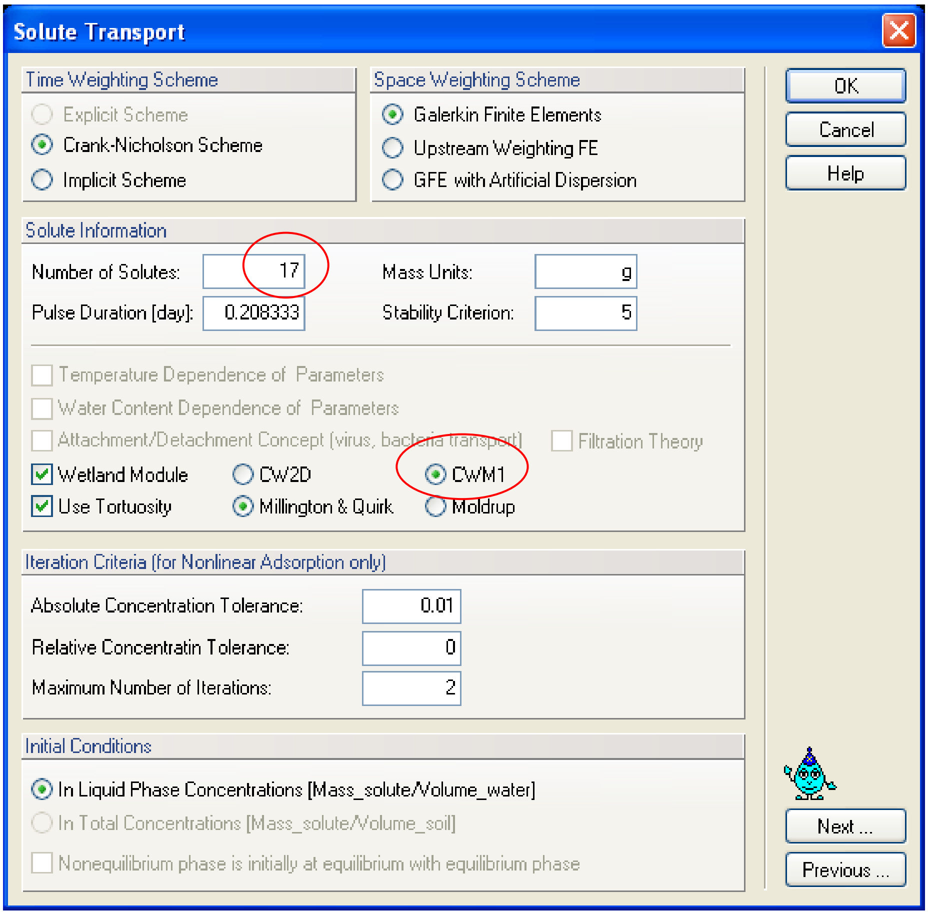


Figure 4.3: The "Solute Transport" window with a selection of the CWM1 biokinetic model.

Please note that the *Iteration Criteria* in the "Solute Transport" window are used to adapt time steps based on the maximum allowed change in the dissolved oxygen concentration ($\Delta c < c_{abs} + c_{rel}.c$) during a particular time step when using the Wetland module (despite the text in the window stating that the iteration criteria are defined *for Nonlinear Adsorption only*). When this criterion is not fulfilled, the next time step will be reduced (see the *dMul2* variable in the HYDRUS technical manual, Šimůnek et al., 2011). Dissolved oxygen is the critical component in both CW2D and CWM1 with respect to their numerical stability as its reaction rates are fastest.

### 4.2.2 The "Solute Transport Parameters" window

Figure 4.4 and Figure 4.5 show the "Solute Transport Parameters" windows for CWM1 and CW2D, respectively. In the "Solute Transport Parameters" window the general transport parameters are set (i.e., bulk density, longitudinal and transverse dispersivities, and diffusion coefficients in the liquid and gaseous phases; for the description of chemical and physical non-equilibrium transport parameters *Fract* and *ThImob* see the HYDRUS manual, Šimůnek et al., 2011).

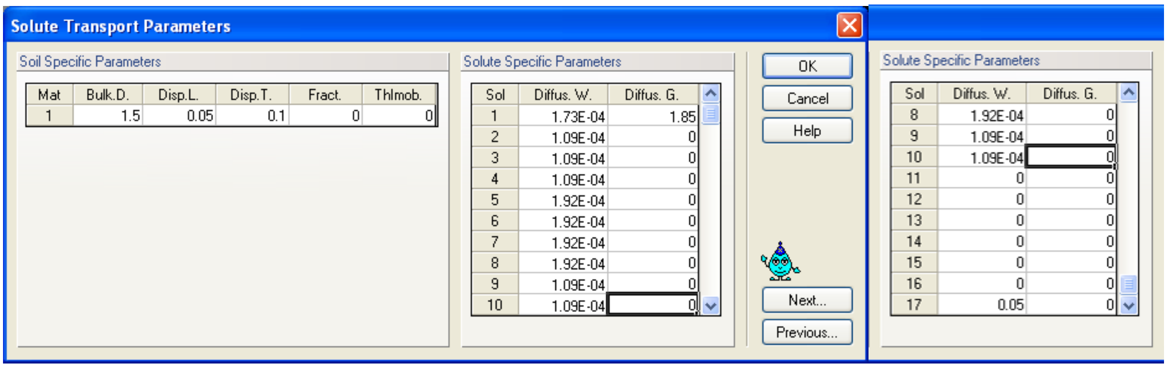


Figure 4.4: The "Solute Transport Parameters" window for CWM1 (for length units in meters and time units in days).

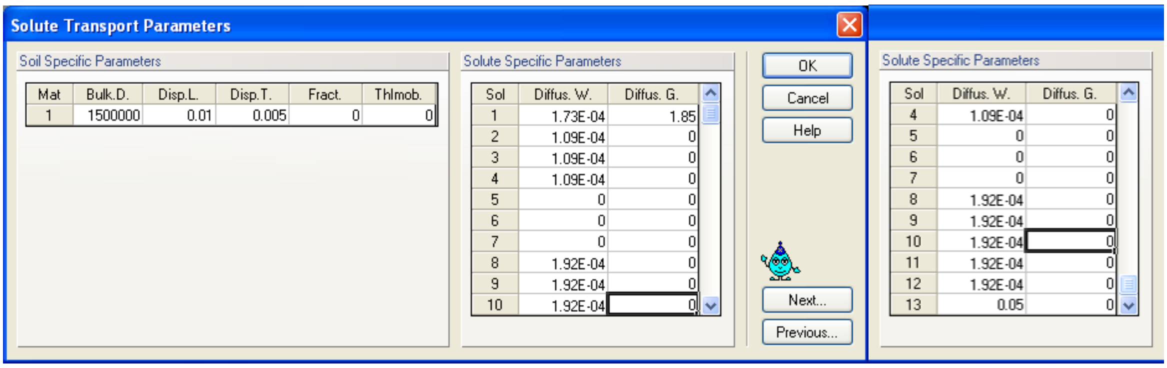


Figure 4.5: The "Solute Transport Parameters" window for CW2D (for length units in meters and time units in days).

Table 4.2 summarises the diffusion coefficients suggested for CW2D and CWM1 compounds. For a comparison with literature data see Langergraber and Šimůnek (2006). The same diffusion coefficient is used for all organic compounds, as well as for all nitrogen compounds. Due to the lack of data, diffusion coefficients for inorganic phosphorus and sulphur compounds are assumed to be the same as for nitrogen.

Table 4.2: Default values of diffusion coefficients for CW2D and CWM1 components (for length units in meters and time units in days).

| **Compound** | **CW2D** | **Liquid** | **Gaseous** | **CWM1** | **Liquid** | **Gaseous** |
|---|---|---|---|---|---|---|
| Dissolved oxygen | SO | 1.73E-04 | 1.85 | SO | 1.73E-04 | 1.85 |
| Organic matter | CR, CS, CI | 1.09E-04 | - | SF, SA, SI, XS, XI | 1.09E-04 | - |
| Ammonium nitrogen | NH4N | 1.92E-04 | - | SNH | 1.92E-04 | - |
| Nitrite nitrogen | NO2N | 1.92E-04 | - | - | - | - |
| Nitrate nitrogen | NO3N | 1.92E-04 | - | SNO | 1.92E-04 | - |
| Elemental nitrogen | N2 | 1.92E-04 | - | - | - | - |
| Phosphate phosphorus | PO4P | 1.92E-04 | - | - | - | - |
| Sulphate sulphur | - | - | - | SSO4 | 1.92E-04 | - |
| Dihydrogensulphide sulphur | - | - | - | SH2S | 1.92E-04 | - |

### 4.2.3 The "Reaction Parameters" window

Figure 4.6 shows the "Reaction Parameters" window for dissolved oxygen. One "Reaction Parameters" window is shown for each defined compound. All CW2D and CWM1 kinetic reactions are implemented as zero-order rate equations separately from the reactions defined in these HYDRUS windows. Therefore all reaction rates in these windows should be zero. Only parameters for the following processes need to be set in these windows:

1. Adsorption and desorption parameters (*Kd*, *Nu*, *Beta*, *Alpha*)
2. Uptake of compounds via roots (*cRoot*)

For the description of these parameters the reader is referred to the HYDRUS manual (Šimůnek et al., 2011).

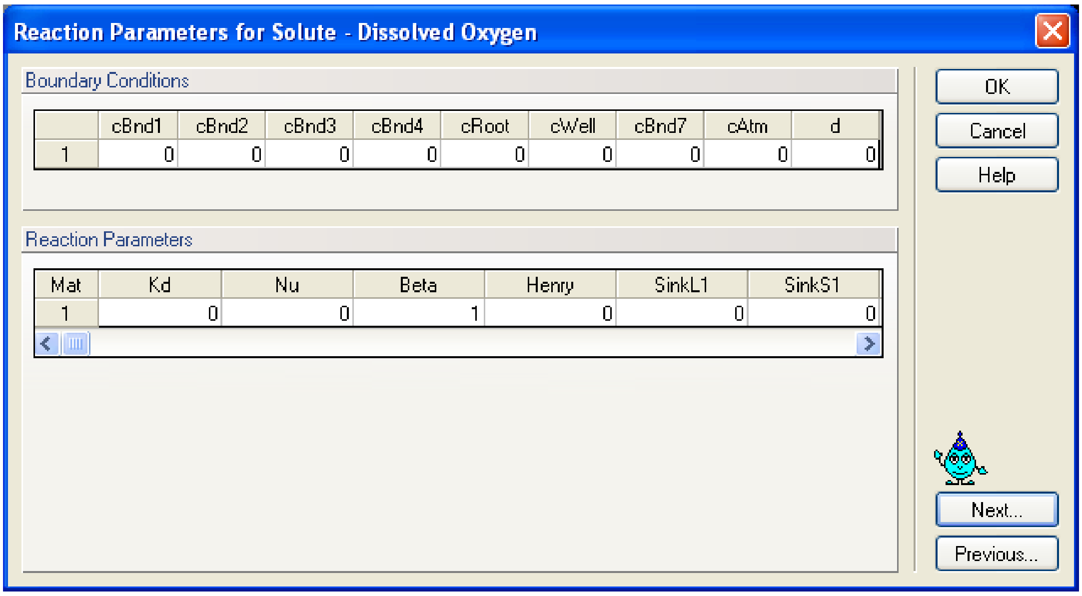


Figure 4.6: The "Reaction Parameters" window.

### 4.2.4 The "Constructed Wetland Model Parameters I" window

The "Constructed Wetland Model Parameters I" and "Constructed Wetland Model Parameters II" windows show the parameters of the biokinetic models, depending on which one is chosen. Figure 4.7 and Figure 4.8 show the kinetic parameters of the CW2D and CWM1 biokinetic models as listed in Table 3.9 and Table 3.15, respectively.

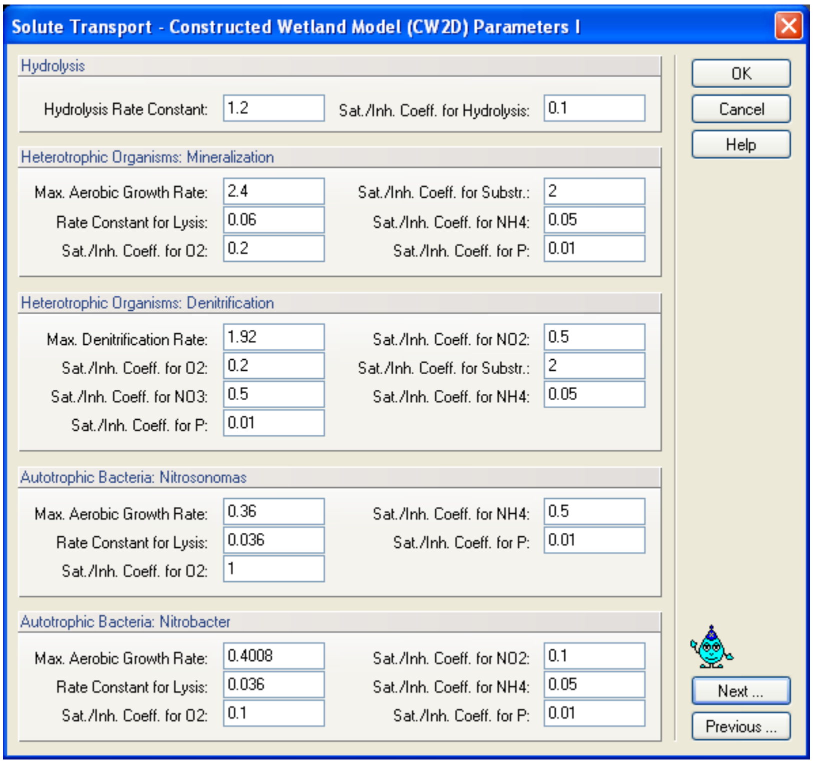


Figure 4.7: The "Constructed Wetland Model (CW2D) Parameters I" window (for time units in days).

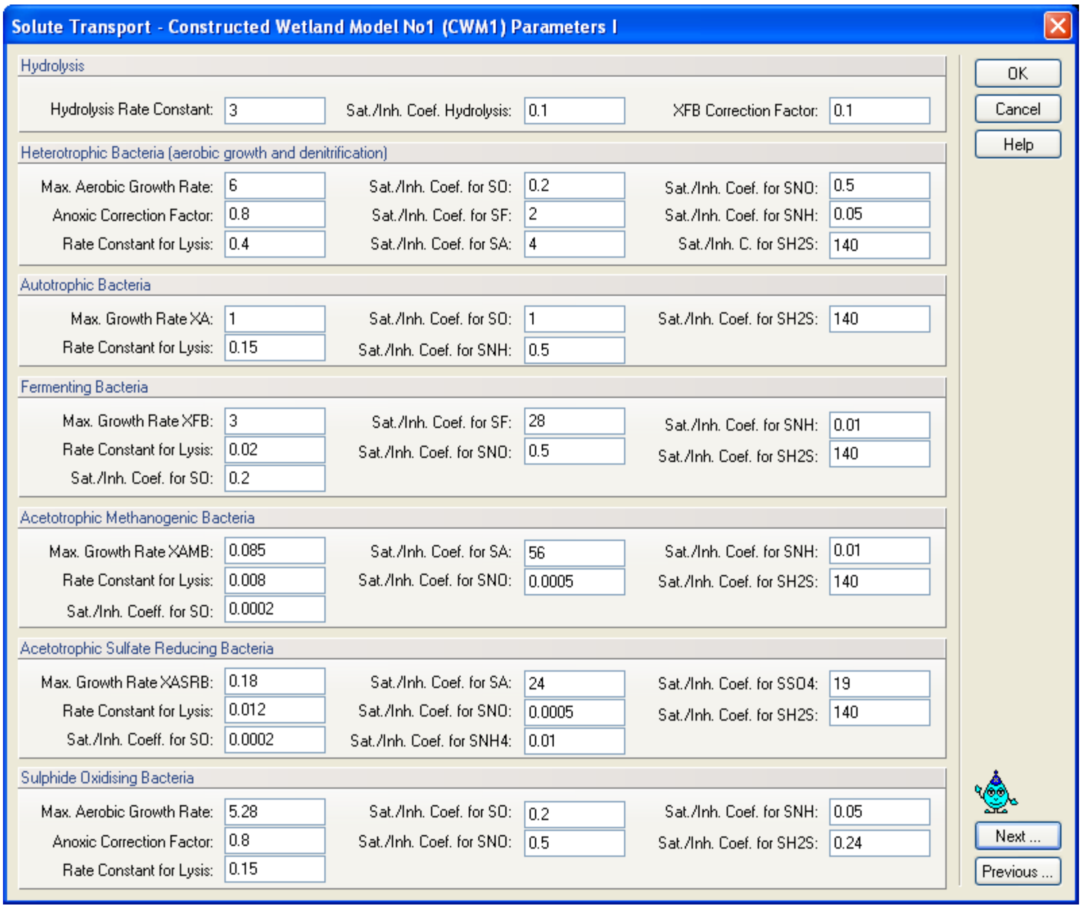


Figure 4.8: The "Constructed Wetland Model No1 (CWM1) Parameters I" window (for time units in days).

### 4.2.5 The "Constructed Wetland Model Parameters II" window

Figure 4.9 and Figure 4.10 show the temperature dependences, stoichiometric parameters, composition parameters, and parameters describing oxygen transfer for the CW2D and CWM1 biokinetic models as listed in Table 3.10 and Table 3.16, respectively.

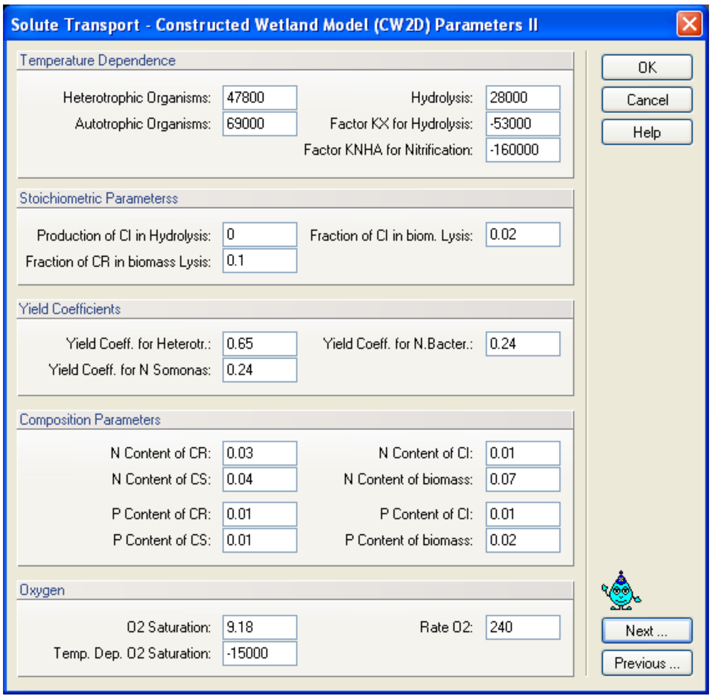


Figure 4.9: The "Constructed Wetland Model (CW2D) Parameters II" window (for time units in days).

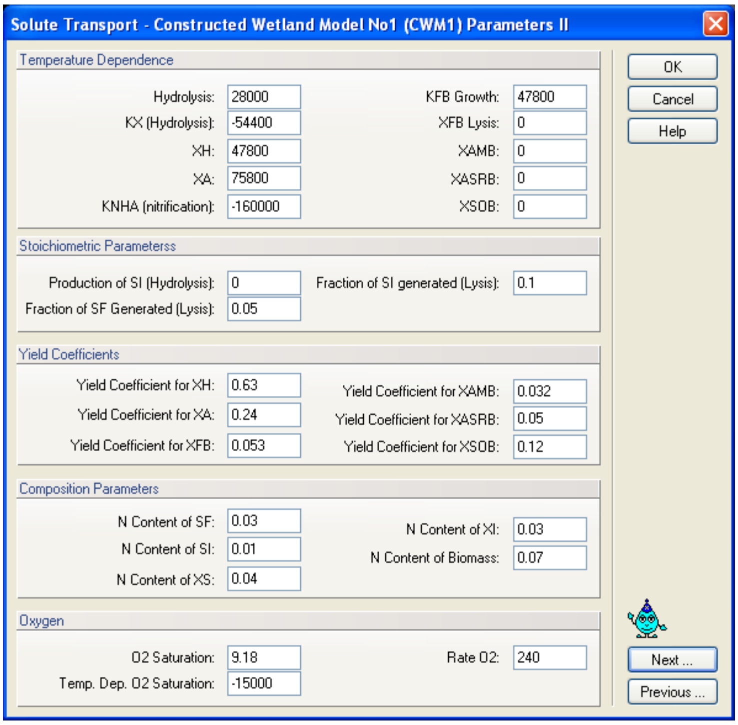


Figure 4.10: The "Constructed Wetland Model No1 (CWM1) Parameters II" window(for time units in days).

### 4.2.6 "Initial Conditions" on the Navigator Bar

Figure 4.11 shows the "Initial Conditions" part of the data tree of the Navigator Bar (the left sidebar of the HYDRUS GUI) for CW2D and CWM1. Names of all components are listed here, with the "L" letter denoting the initial concentration in the liquid phase and "S" the initial concentration in the solid phase. The names of the same components also appear when importing initial conditions from previous simulation runs, as shown in Figure 4.12 for CWM1.

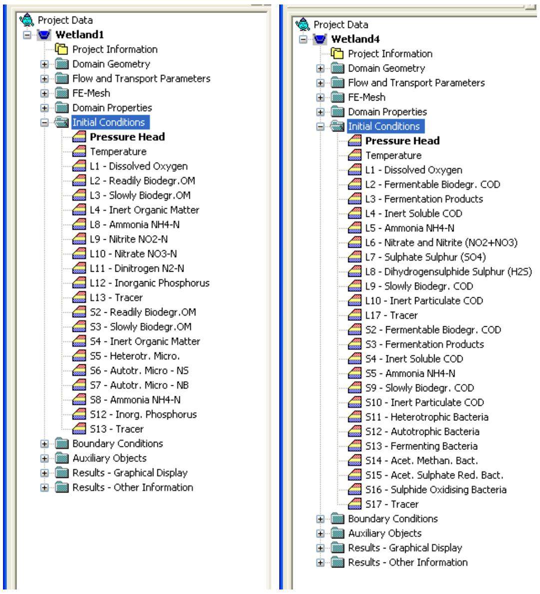


Figure 4.11: "Initial Conditions" in the data tree of the Navigator Bar for CW2D (left) and CWM1 (right).

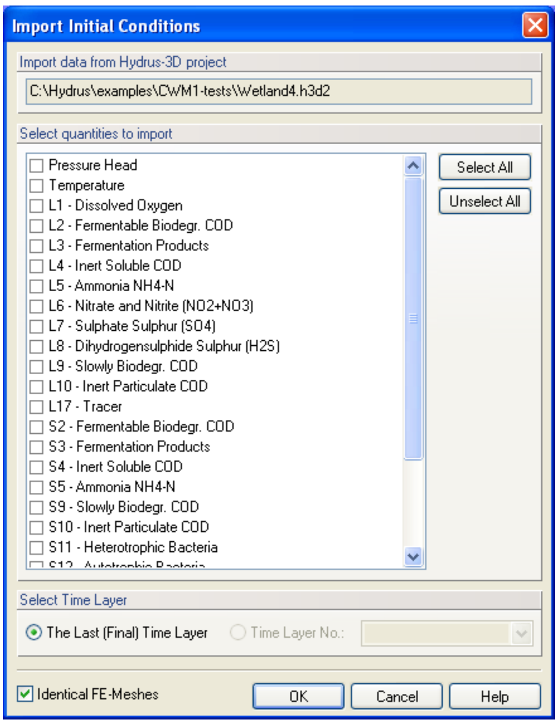


Figure 4.12: The "Import Initial Conditions" window for CWM1.

## 4.3 Post-processing

### 4.3.1 The "Results - Graphical Display" window

Figure 4.13 and Figure 4.14 show the main window of the HYDRUS GUI with the "Results - Graphical Display" section of the Navigator Bar open for CW2D and CWM1, respectively. In both figures the concentration of heterotrophic organisms is shown. Similarly as when defining the initial conditions, the names of all components are listed in this section of the Navigator Bar.

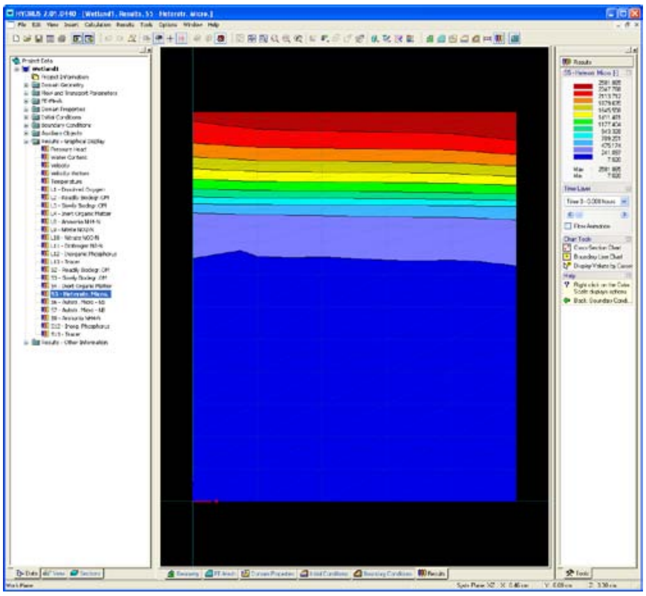

Figure 4.13: The main window of HYDRUS GUI for CW2D with the "Results - Graphical Display" section of the Navigator Bar open.

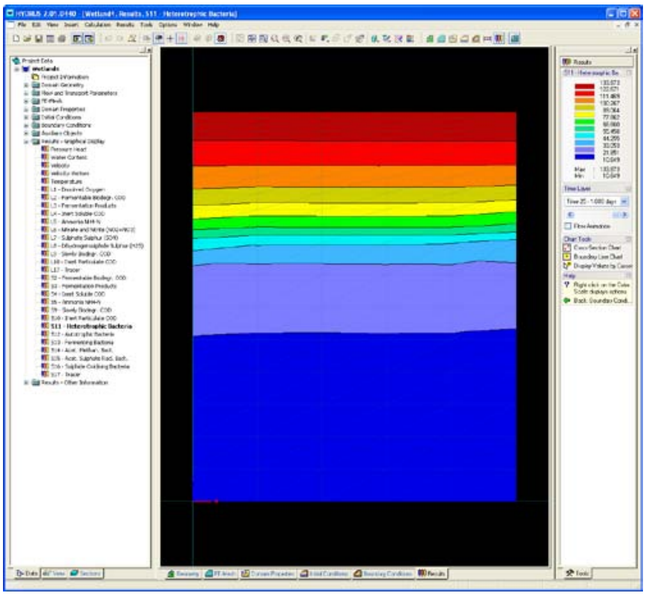

Figure 4.14: The main window of HYDRUS GUI for CWM1 with the "Results - Graphical Display" section of the Navigator Bar open.

## 4.3.2 The "Observation Nodes" window

Figure 4.15 and Figure 4.16 show the "Observation Nodes" window for CW2D and CWM1, respectively. Again names of all variables are displayed, including all biochemical compounds.

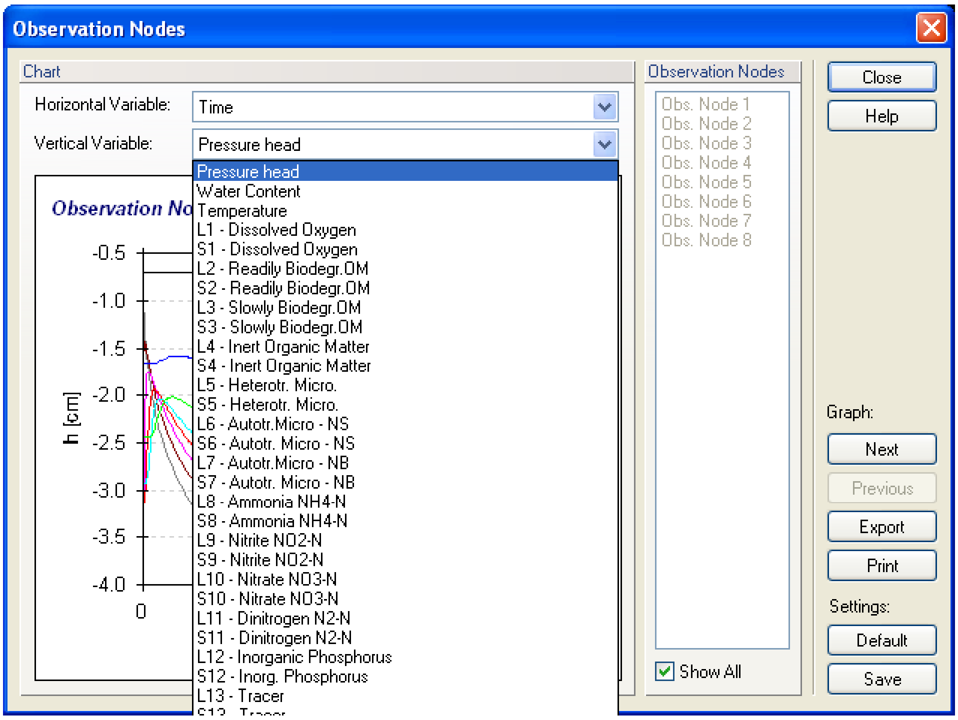


Figure 4.15: The "Observation Nodes" window for CW2D.

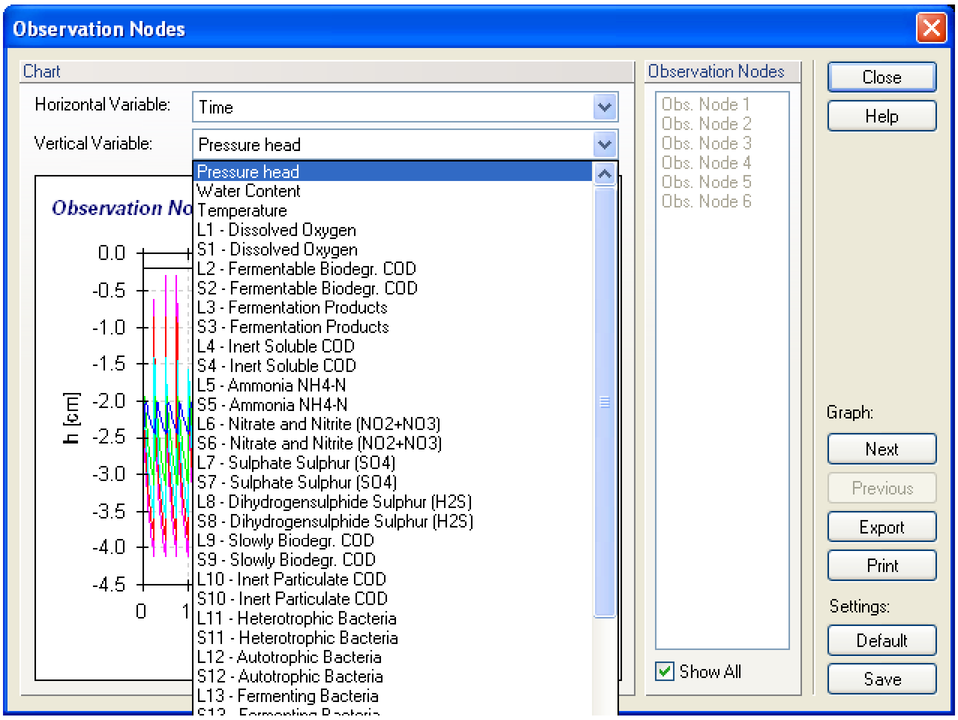


Figure 4.16: The "Observation Nodes" window for CWM1.

# 5 Examples

## 5.1 Pilot-scale vertical flow CW for wastewater treatment (*Wetland 4*)

The *Wetland 4* example is the same as the *Wetland* 1 example described in Chapter 5.1 of the manual for version 1 of the HYDRUS wetland model (Langergraber and Šimůnek, 2006), except evaluated using the CWM1 model instead of the CW2D biokinetic model. In the following text, the steps needed to set-up *Wetland 4* from *Wetland 1* are shown. To ensure that all other factors (e.g., transport domain, FE-mesh, water flow) of this project remain the same and only the reactive transport parameters are changed we start by copying the *Wetland 1* project and rename it *Wetland 4* (Figure 5.1). Note that in *Wetland 1* the length units were centimeters and the time units were hours and that they remain the same in *Wetland 4*. After opening the project, we change the biokinetic model from CW2D to CWM1 in the "Solute Transport" window (Figure 5.2).

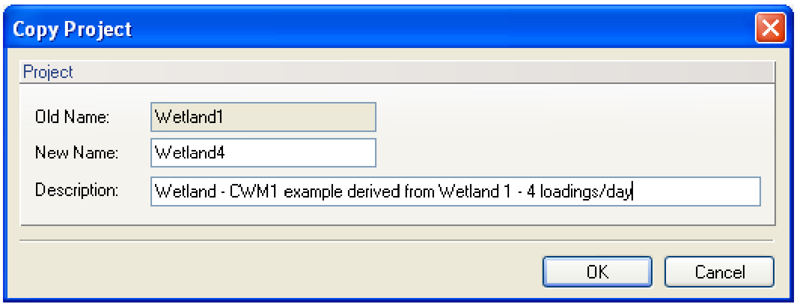


Figure 5.1: The "Copy Project" window.

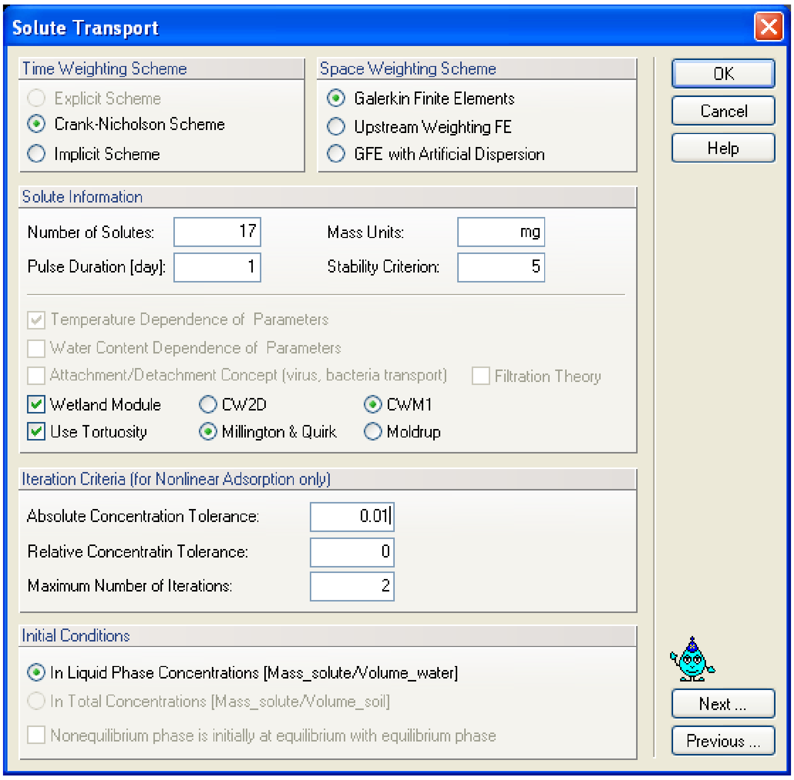


Figure 5.2: Selection of the biokinetic model in the "Solute Transport" window.

In the next step the diffusion coefficients must be specified in the "Solute Transport Parameters" window (Figure 5.3), e.g., to default values as shown in Figure 4.4.

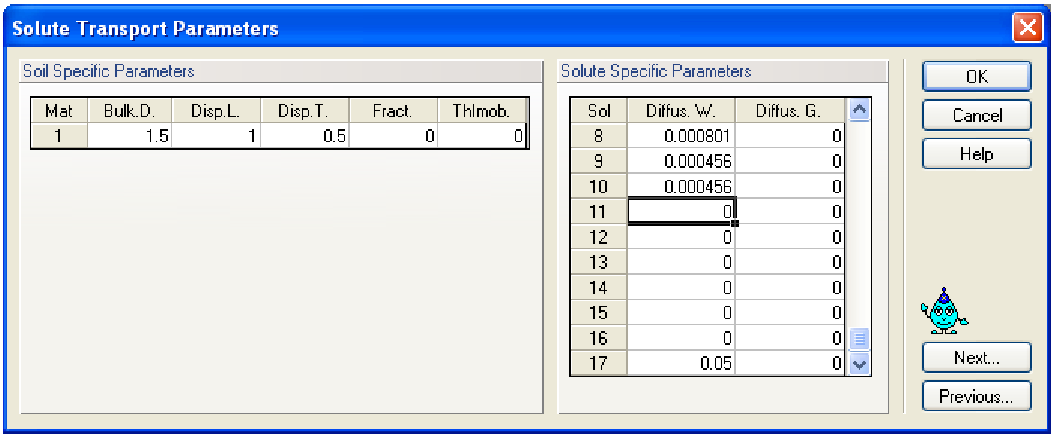


Figure 5.3: Set up of diffusion coefficients in the "Solute Transport Parameters" window.

In *Wetland 1*, adsorption was considered for phosphorus and the tracer compound (CW2D components 12 and 13, respectively). In the "Reaction Parameters" window (Figure 4.6) the adsorption parameters have to be checked and the parameters $K_d$ and *Alpha* have to be set to 0 for CWM1 components 12 through 16.

The next step is to specify the influent concentrations in the "Time Variable Boundary Conditions" window. The COD fractionation, i.e., the distribution of the total COD between individual COD model fractions, has to be done. A comparison between organic matter components in CW2D and CWM1 is shown in Table 5.1. It is assumed that CI = SI + XI (the inert fraction is the same); CS = XS; and CR = SF+SA (mostly SF) (Table 5.1).

Table 5.1: COD influent fractionation for organic matter components in CW2D and CWM1 for a total COD of 300 mg/L (values in mg/L).

| **CW2D components** | **CR** | **CS** | **CI** | | |
|---|---|---|---|---|---|
| **Value** | 160 | 120 | 20 | | |
| **CWM1 components** | **SF** | **SA** | **SI** | **XS** | **XI** |
| **Value** | 155 | 5 | 10 | 120 | 10 |

Table 5.2 shows the influent concentrations used for the *Wetland 4* example. Figure 5.4 shows where and how to specify the influent concentrations of individual components (note that component 17 is an independent tracer; also note that in *cValx-y*, *x* is the BC number and *y* is the component number). Similarly as in *Wetland 1*, cValue2, i.e., the 2nd vector of the time-dependent solute concentrations, is used in *Wetland 4* as well.

Table 5.2: Influent concentrations (values in mg/L).

| **Components** | **SO** | **SF** | **SA** | **SI** | **SNH** | **SNO** | **SSO4** | **SH2S** | **XS** | **XI** |
|---|---|---|---|---|---|---|---|---|---|---|
| **Value** | 1 | 155 | 5 | 10 | 60 | 0.1 | 20 | 0.1 | 120 | 10 |

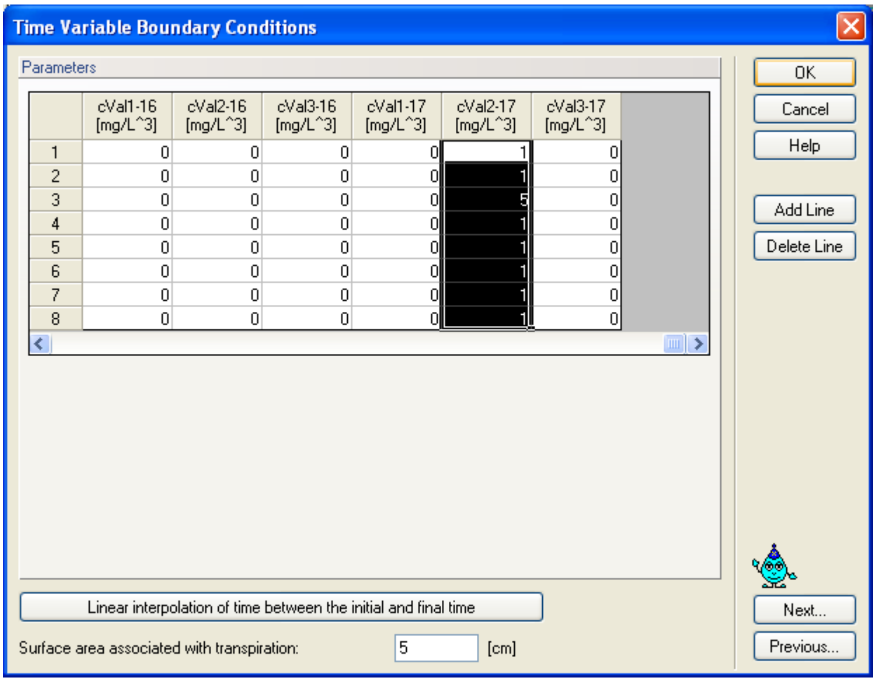


Figure 5.4: Inflow concentrations in the "Time Variable Boundary Conditions" window.

The next step is to set initial conditions for the CWM1 components (note that this Table, i.e., "Default Domain Properties", is available only for simple rectangular geometries and that for general geometries, one needs to define initial conditions graphically). A simple approach to set the initial conditions is chosen: all liquid and solid phase concentrations are set to 1 if the component is considered or to 0 if not, i.e. for *Wetland 4* this results in: L1-L10 =1; L11-L16 =0; L17 =1; S1-10 =0 and S11-17 =1 (Figure 5.5). Although 13 or 17 components are displayed in this table for CW2D and CWM1 modules, initial values need to be specified only for those, which are needed as shown in Table 3.3.

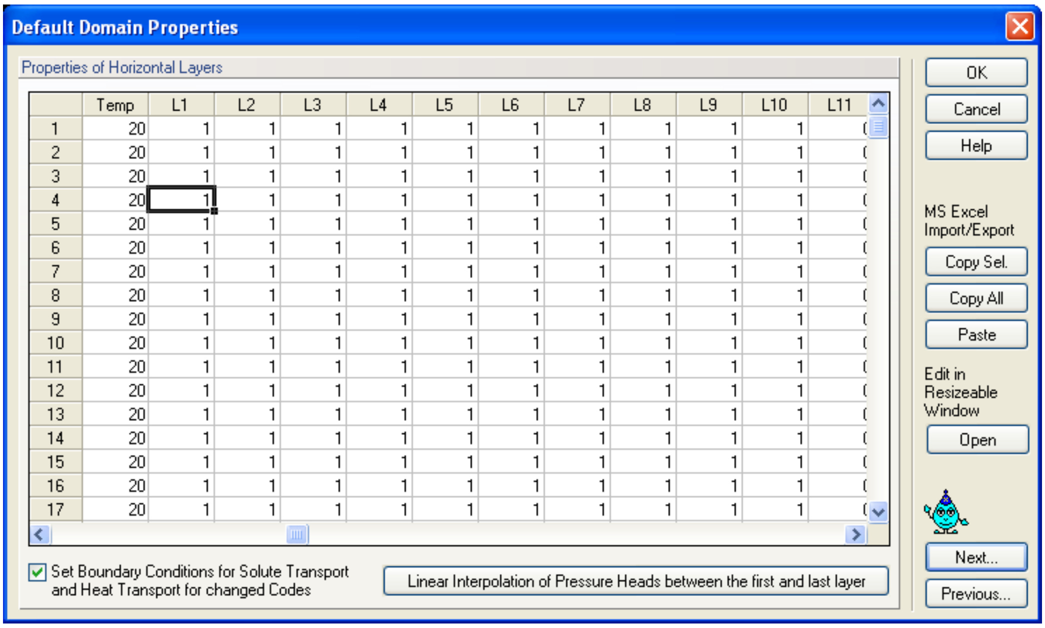


Figure 5.5: The "Default Domain Properties" window.

Finally, since we want to run the simulation for 10 days we have to adjust the Final Time in the "Time Information" window (Figure 5.6). Since we want to repeat the same loading pattern each day, the *Number of times to repeat the same set of BC records* is therefore set to 10. The *Maximum Time Step* is 60 seconds. Together with the settings for iteration criteria in the "Solute Transport" window (Figure 5.2), the *Maximum Time Step* defines the stability of the numerical solution (see before). For *Wetland 4* with a *Maximum Time Step* of 60 seconds, an *Absolute Concentration Tolerance* of 0.01 mg/L is a setting that avoids numerical instabilities.

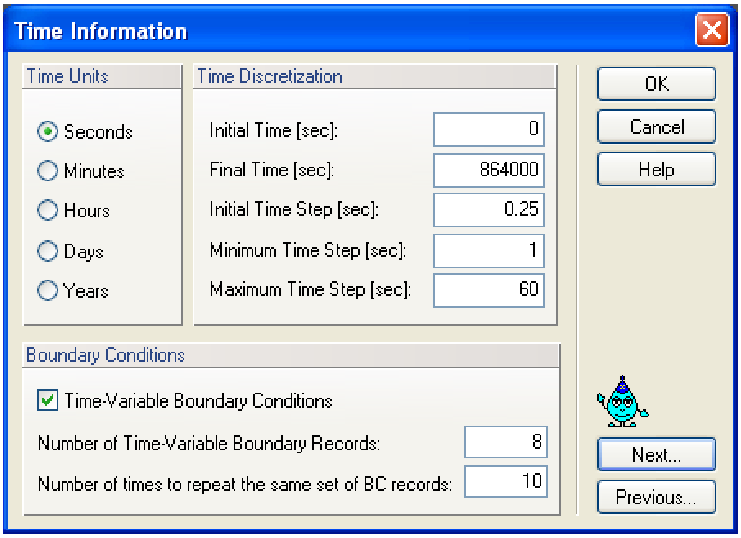


Figure 5.6: The "Time Information" window.

Figure 5.7 through Figure 5.10 show the simulation results at 5 observation nodes during the first 10 days for fermentable soluble COD (SF), nitrate nitrogen (SNO), heterotrophic bacteria (XH), and autotrophic bacteria (XA), respectively. The observation nodes have been set at depths of 1, 5, 10, 25, and 60 cm in the vertical flow filter. The observation node at the 60-cm depth (#1) represents the effluent concentration. Please note that simulation results obtained by CWM1 for this example have not been verified using measured data.

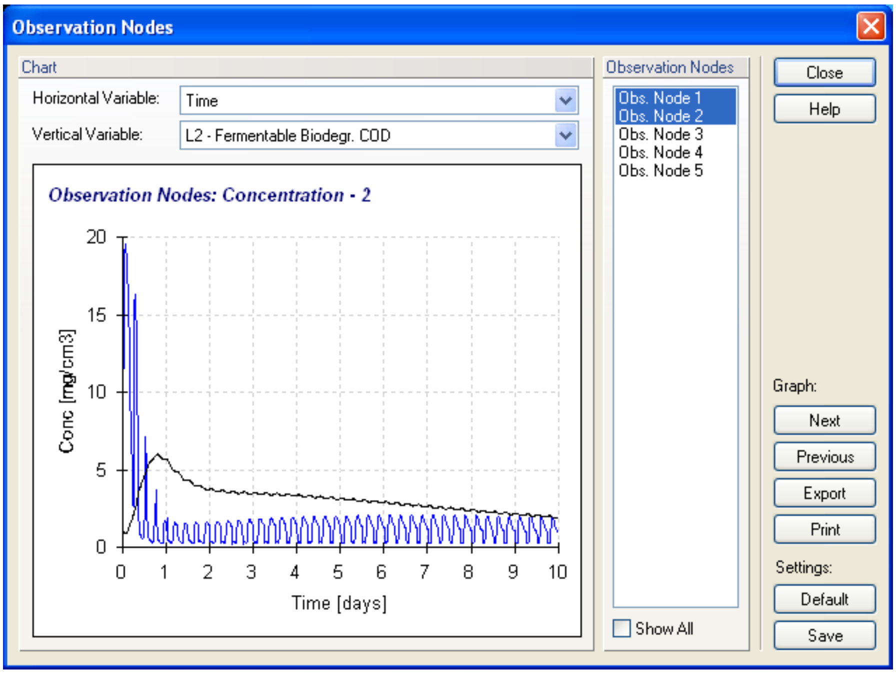


Figure 5.7: Concentrations of fermentable, readily biodegradable soluble COD (SF) at 2 depths (the *Wetland 4* example).

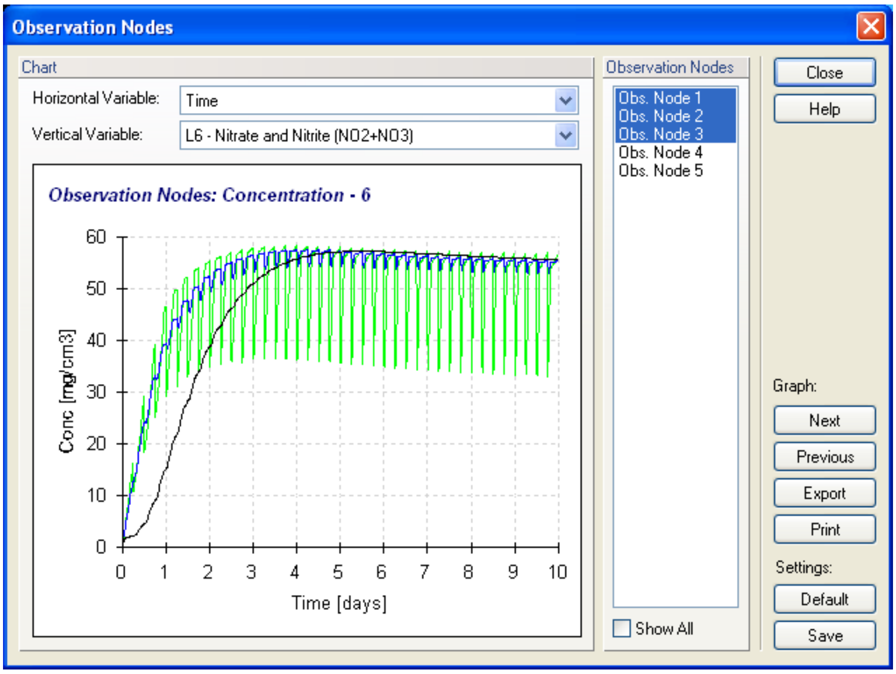


Figure 5.8: Concentrations of nitrate nitrogen (SNO) at 3 depths (the *Wetland 4* example).

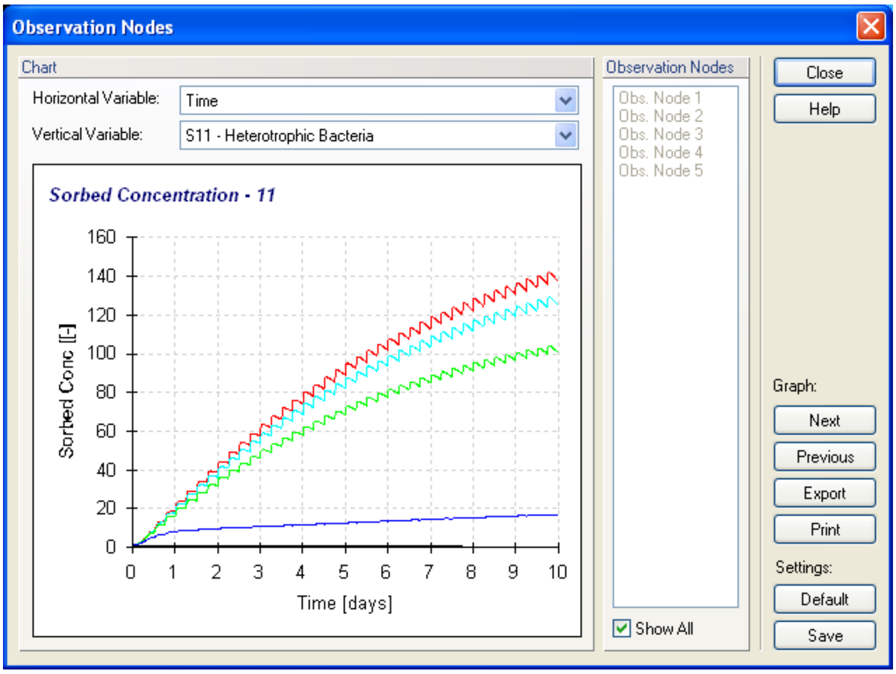


Figure 5.9: Concentrations of heterotrophic bacteria (XH) at 5 depths (the *Wetland 4* example).

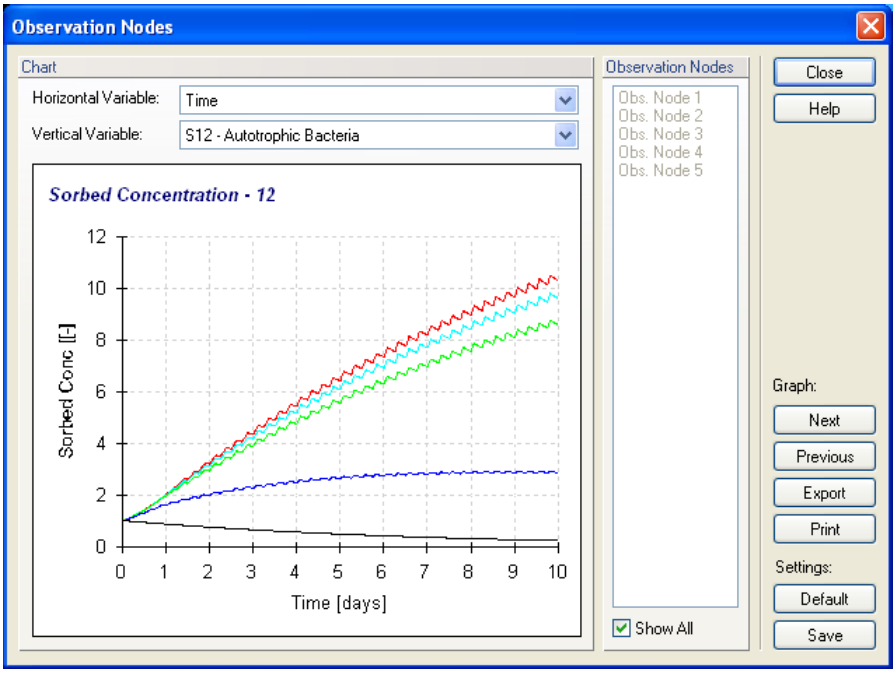


Figure 5.10: Concentrations of autotrophic bacteria (XA) at 5 depths (the *Wetland 4* example).

## 5.2 Pilot-scale horizontal flow CW for wastewater treatment (*Wetland 5*)

### 5.2.1 System description and measured data

The *Wetland 5* example is based on the experiments for a HF CW described by Headley et al. (2005). The experimental site consisted of a 1 m deep HF CW planted with *Schoenoplectus tabernaemontani* (soft stem bulrush) and was designed to treat primary settled municipal wastewater in sub-tropical New South Wales, Australia. Water samples were collected from the upper (0.17 m), middle (0.5 m), and lower (0.83 m) depths at five equally-spaced sample points along the longitudinal axis of the 8.8 $m^2$ bed (Figure 5.11). Figure 5.12 shows measured data for $BOD_5$ and $NH_4$ concentrations measured along the flow path of the HF CW obtained at a hydraulic loading rate of 40 mm/d.

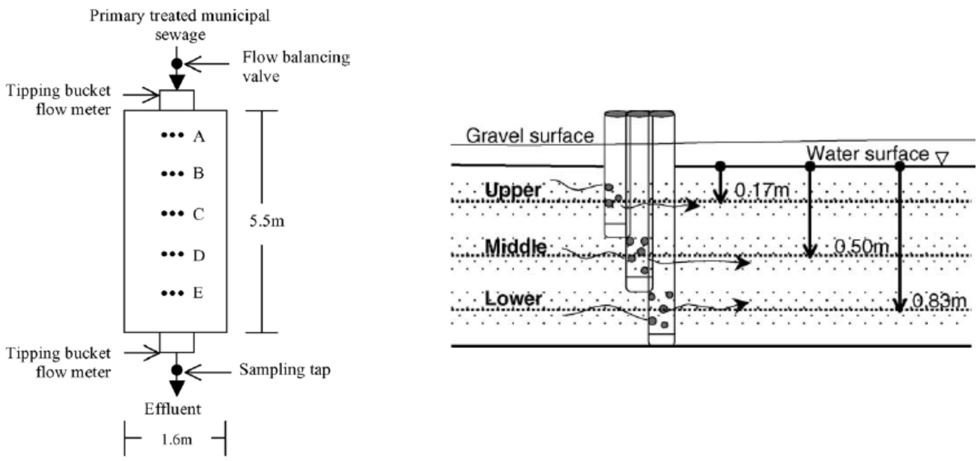


Figure 5.11: Plan view of the HF CW showing sampling wells (left) and a cross-sectional view of one of five intermediate sampling wells (right) (Headley et al., 2005).

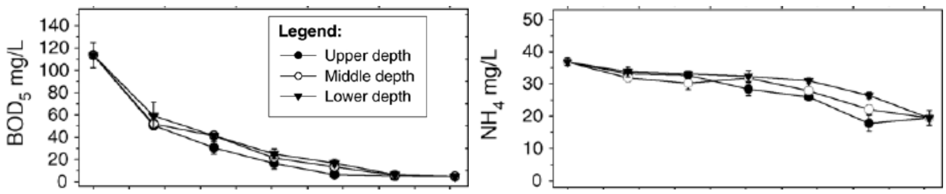


Figure 5.12: $BOD_5$ and $NH_4$ concentrations measured along the flow path of the HF CW (Headley et al., 2005).

### 5.2.2 Model set-up

The width of the transport domain was 5.5 m, its depth was 1.1 m (1 m bed depth and 0.1 m free board are simulated), and the slope of the domain was 0.1°. The transport domain itself was discretized into 37 columns and 26 rows. This resulted in a structured two-dimensional finite element mesh consisting of 926 nodes and 1800 triangular finite elements. As described by Headley et al. (2005), the first 0.5 m on the right part of the domain is a distribution zone (a right part of Figure 5.13) that consists of a different material than the main bed. An atmospheric BC is used at the inlet point (a top right part in Figure 5.13) and a constant pressure head BC (a constant head of 95 cm at a node 5 cm above the bottom of the domain) at the outlet point (bottom left in Figure 5.13) of the system. This guarantees that the water level in the HF bed is maintained at 1 m. Calculations for *Wetland 5* have been carried out using the CW2D biokinetic model. Using instead the CWM1 biokinetic model can be done as described in *Wetland 4*.

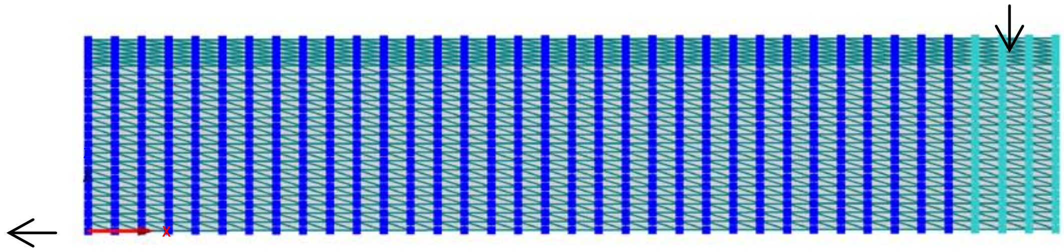

Figure 5.13: Material distribution (right: inlet distribution zone = Material 2).

Headley et al. (2005) reported that the root biomass was very dense in the upper 25 cm of HF bed, decreased rapidly with depth, and only very few roots were observed at depths greater than 40 cm below the surface. The root distribution was set up accordingly (Figure 5.14). Note that no roots are present in the inlet distribution zone.

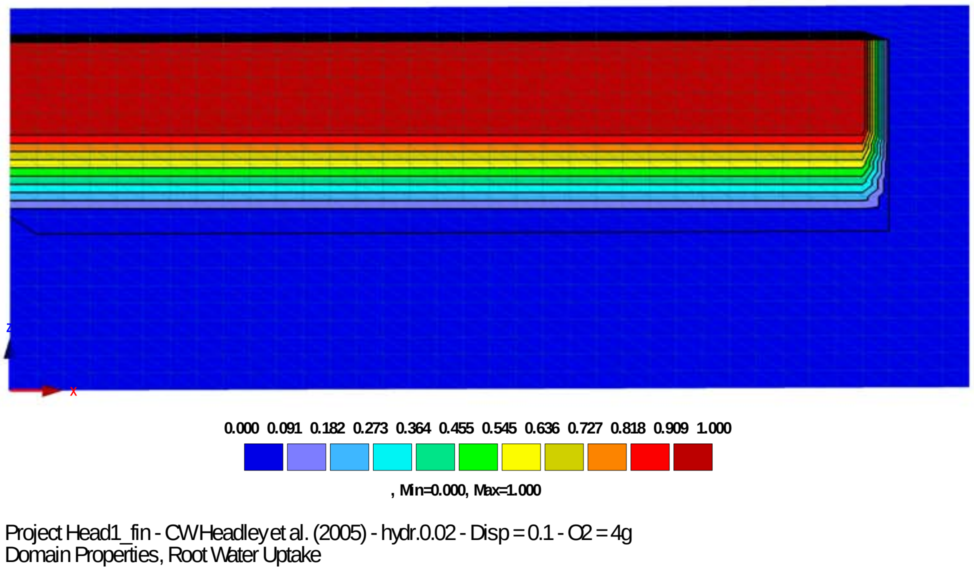


Figure 5.14: Root water uptake distribution.

Parameters for root water and solutes uptake are shown in Table 5.3 and the settings in the GUI in Figure 5.15 through Figure 5.17. The negative value of *cRoot* for Dissolved Oxygen is used to model oxygen release from the plant roots.

Table 5.3: Parameters for root water and solutes uptake.

| **Parameter** | **Value** | **Unit** | **Window** |
|---|---|---|---|
| Potential transpiration rate | 0.0115 | m/h | Time Variably Boundary Conditions (Figure 5.15) |
| *cRoot* (Ammonia NH4) | 50 | g/m³ | Reaction Parameters for NH4 (Figure 5.16) |
| *cRoot* (Dissolved Oxygen) | -800 | g/m³ | Reaction Parameters for Oxygen (Figure 5.17) |

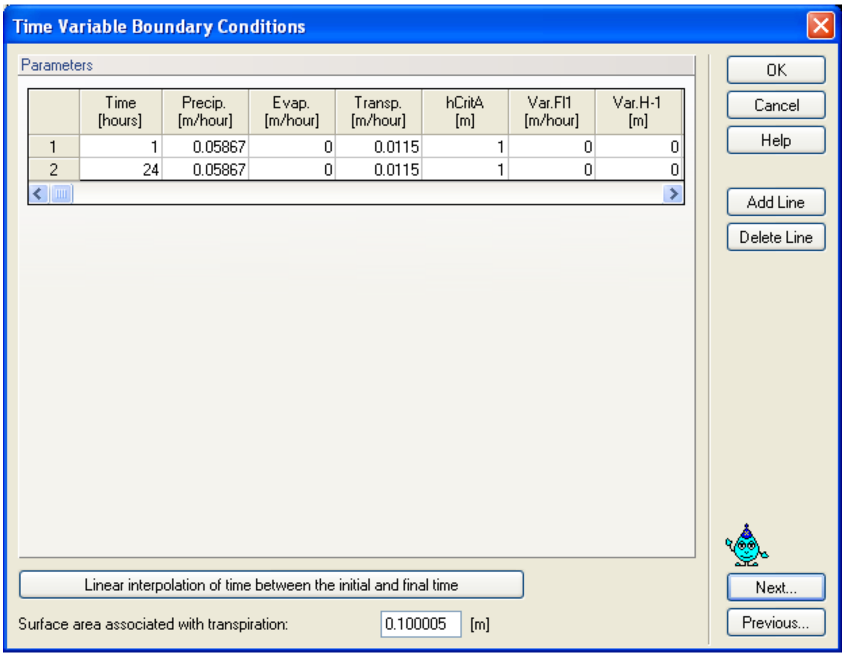


Figure 5.15: The "Time Variable Boundary Conditions" window.

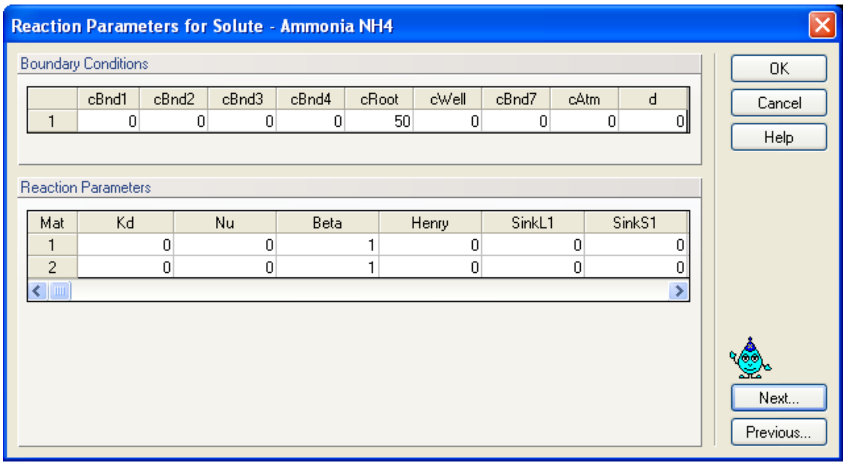


Figure 5.16: The Ammonia NH4 "Reaction Parameters" window.

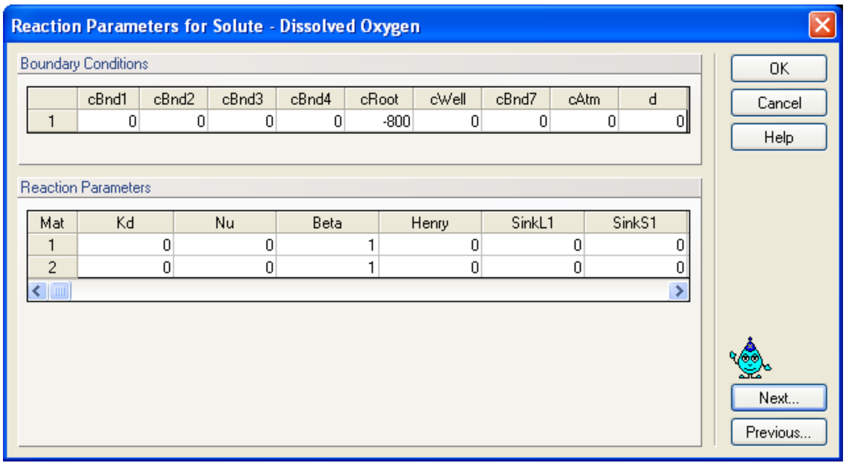


Figure 5.17: The Dissolved Oxygen "Reaction Parameters" window.

### 5.2.3 Simulation results

Figure 5.18 shows the cumulative oxygen release by plant roots for a simulation time of 1 day. The simulated cumulative release is 20 g/m (a minus value for uptake indicates a release of oxygen). This results in a specific oxygen release of 2.5 g/m²/d (the total area covered by plants is 8 m² (5 m length of the bed times 1.6 m width), a rather conservative value. However, this oxygen release resulted in dissolved oxygen concentrations of about 0.1 mg/L in the root zone near the outlet of the bed (Figure 5.19 and Figure 5.20). Note that the contour levels in Figure 5.19 were adjusted to emphasize small values. Only by considering oxygen release by plant roots it was possible to simulate the decrease of $NH_4$-N concentrations along the flow path in the HF bed (Figure 5.21). Figure 5.22 and Figure 5.23 show that the simulation results are in good agreement with measured data for $NH_4$-N and COD concentrations, respectively.

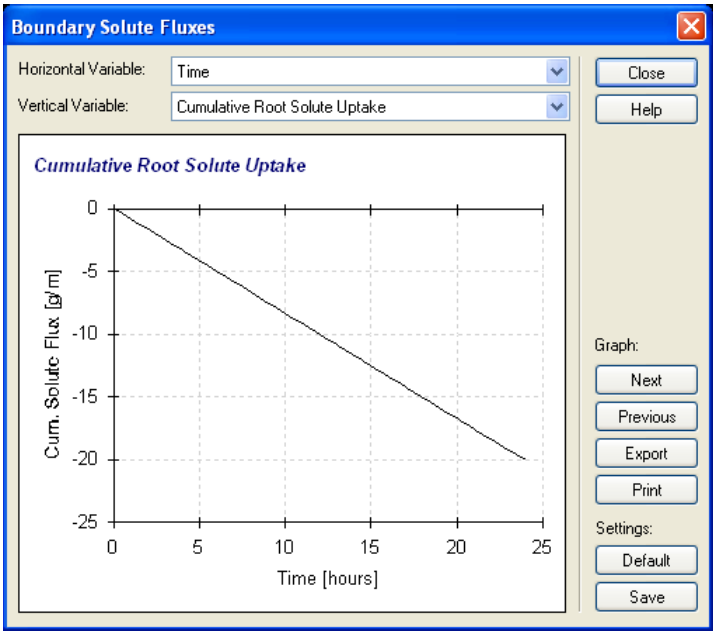


Figure 5.18: Cumulative Root Solute Uptake for Dissolved Oxygen.

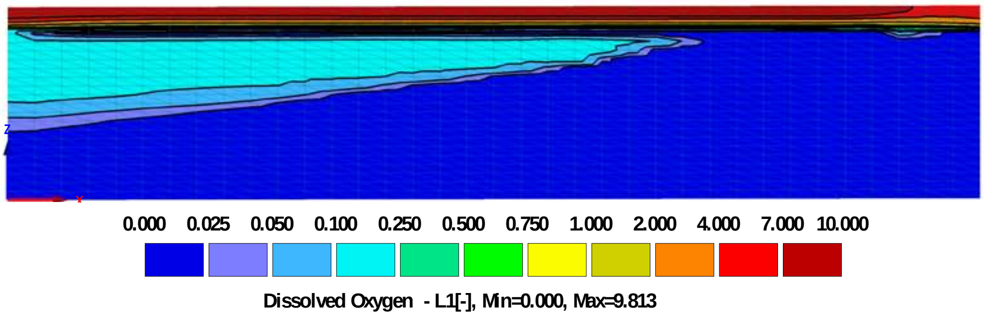


Figure 5.19: Dissolved Oxygen concentrations in the two-dimensional domain.

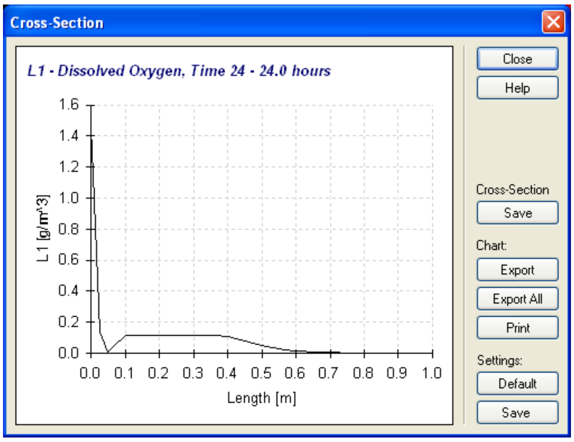


Figure 5.20: Dissolved Oxygen concentrations in a vertical cross section through the HF bed 0.5 m before the effluent.

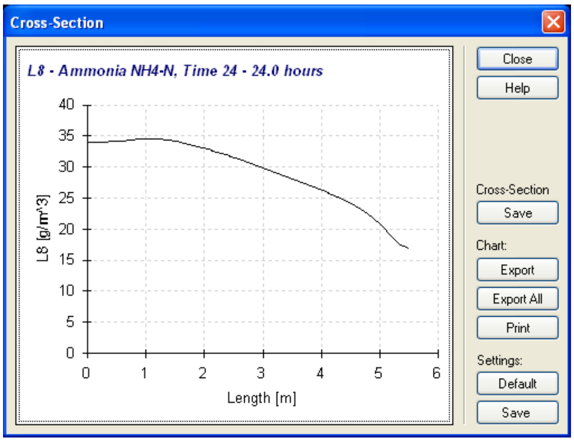


Figure 5.21: NH4-N concentrations along the flow path in a depth of 50 cm in the HF bed.

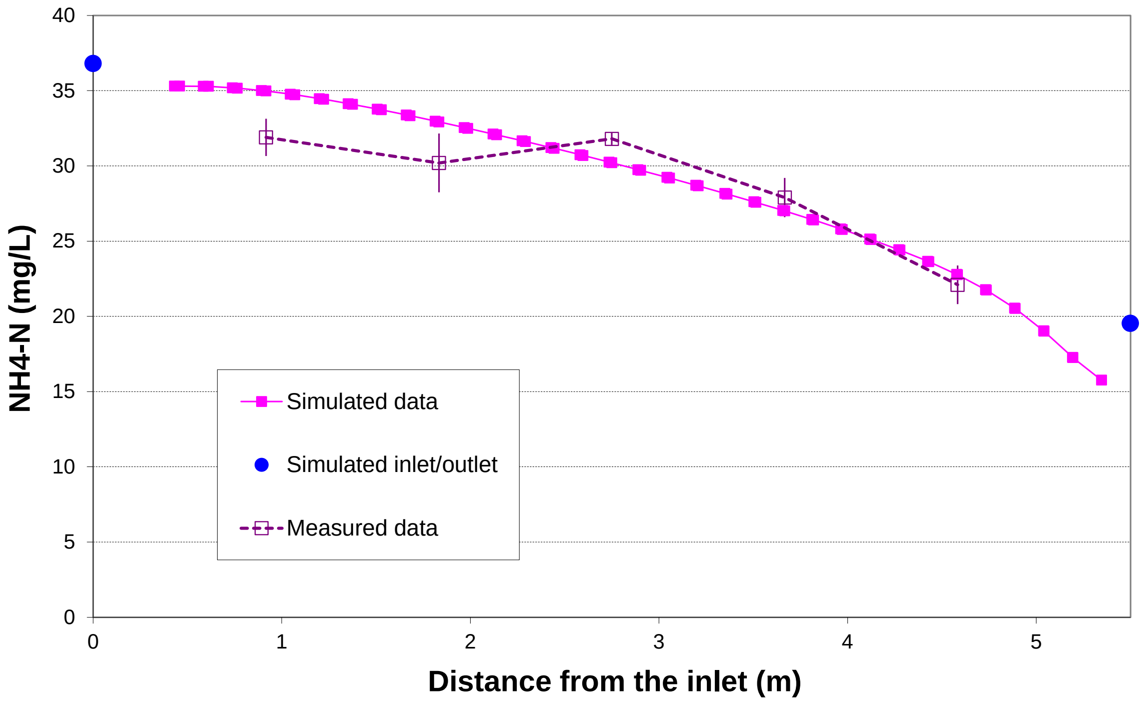


Figure 5.22: Comparison of measured and simulated $NH_4$-N concentrations along the flow path in a depth of 50 cm of the HF bed.

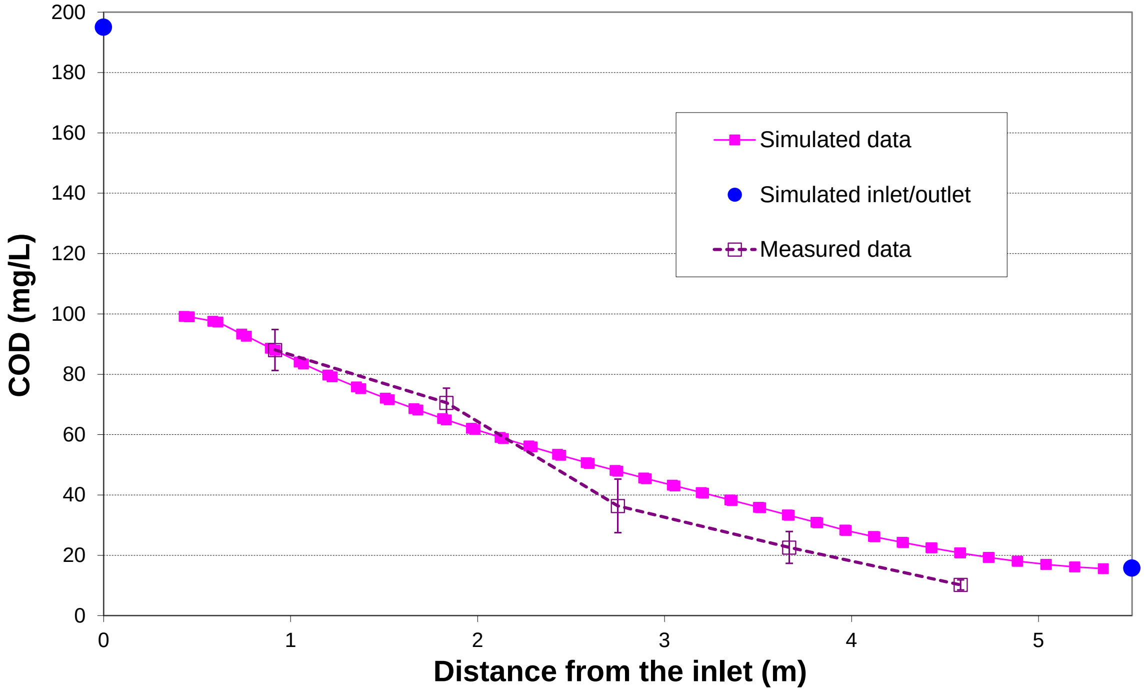


Figure 5.23: Comparison of measured and simulated COD concentrations along the flow path in a depth of 50 cm of the HF bed.

## 5.3 Applications of the HYDRUS wetland module

The following list gives an overview of different applications, in which the HYDRUS wetland module was used:

- CWs for treating combined sewer overflow (compare example "*Wetland 3*" as described in chapter 5.3 of Langergraber and Šimůnek, 2006): Dittmer et al. (2005), Henrichs et al. (2007, 2009), and Meyer et al. (2008).
- CWs treating effluents of the wastewater treatment plant for irrigation purposes: Toscano et al. (2009).
- Simulating run-off from agricultural sites and the effect of streamside management zones: Smethurst et al. (2009, 2010).

# 6 Input data

## 6.1 The 'options.in' input file

An additional option, namely limited effluent flow rates, can be specified in the additional input file 'options.in'.

The 'options.in' input file is not supported by the graphical user interface of the HYDRUS software. It needs to be created manually and placed in the temporary working directory created by HYDRUS (Šimůnek et al., 2011). If this input file does not exist, then HYDRUS does not consider this additional option (note that this file was more extensive in the past, but a lot of the special options in version 1 have become standard features in version 2).

The definition of variables used in 'options.in' is given in Table 6.1, and an example of the file is given below:

```
Input file "Options.in"
lSeepLimit   qSLimit (positive)
f            0.
```

Table 6.1: Description of variables used in the 'options.in' input file.

| Variable name | Type | Unit | Description |
|---|---|---|---|
| lSeepLimit | logical | - | = true: use the maximum effluent flow rate for a seepage face BC;<br>= false: normal seepage face BC |
| qSLimit | float | [L/T] | Maximum allowed seepage face flux (positive) |

# 7 Output data

## 7.1 Format of the `'effluent.out'` output file

An additional output-file `'effluent.out'` is created that contains information about effluent concentrations along the outflow boundary. If multiple outflow boundaries exist, only the concentration value for the first boundary from this list (free drainage boundary, seepage face boundary, variable flux boundary, and constant flux boundary) is printed. This file is printed during the simulation run.

```
All solute fluxes and cumulative solute fluxes are positive out of the region

      Time       cEff(1)       cEff(2)      ...   cEff(12)      cEff(13)     TempEff

     .0000010   .870194E+01   .227306E+00  ...  .162806E+01   .138496E+01     20.0000
     .0009541   .870195E+01   .227296E+00  ...  .162805E+01   .138496E+01     20.0000
     .0033000   .870198E+01   .227269E+00  ...  .162804E+01   .138496E+01     20.0000
     :
     :
```

The `'effluent.out'` output file can be found in the temporary working directory created by HYDRUS (Šimůnek et al., 2011).

# 8 List of examples

**For CW2D**

For the description of the CW2D examples see Langergraber and Šimůnek (2006).

**a) Wetland1**

A pilot-scale vertical flow constructed wetland (PSCW, chapter 5.1 in Langergraber and Šimůnek, 2006); an example of flow and reactive transport simulations.

**b) Wetland2**

A two-stage vertical flow constructed wetland (SSP, chapter 5.2 in Langergraber and Šimůnek, 2006); an example of reactive transport simulations.

**c) Wetland3**

A lab-scale vertical flow constructed wetland for treatment of combined sewer overflow (CSOCW, chapter 5.3 in Langergraber and Šimůnek, 2006); an example for controlled effluent rate.

**d) Wetland5**

An experimental HF CW described by Headley et al. (2005); an example for simulating the influence of wetland plants (see chapter 5.2 of this manual).

**For CWM1**

**e) Wetland4**

Same as Wetland 1 but using the CWM1 biokinetic model; an example of how to start a simulation using the new CWM1 biokinetic model (see chapter 5.1 of this manual).

# 9 References


Brovelli, A., Baechler, S., Rossi, L., Barry, D.A. (2009a): Comprehensive process-based modelling of sand filters and subsurface flow constructed wetlands. In: Bayona, J.M., García, J. (Eds.): *3rd International Symposium on "Wetland Pollutant Dynamics and Control – WETPOL 2009" – Book of Abstracts*, 20-24 September 2009, Barcelona, Spain, pp. 293-294.

Brovelli, A., Malaguerra, F., Barry, D.A. (2009b): Bioclogging in porous media: Model development and sensitivity to initial conditions. *Environ Model Softw* 24(5), 511-25.

Chen, S., Wang, G.T., Xue, S.K. (1999): Modeling BOD removal in constructed wetlands with mixing cell method. *J Environ Eng* 125(1), 64-71.

Corominas, L., Rieger, L., Takács, I., Ekama, G., Hauduc, H., Vanrolleghem, P.A., Oehmen, A., Gernaey, K.V., Comeau, Y. (2010): New framework for standardized notation in wastewater treatment modelling. *Water Sci Technol* 61(4), 841-857.

Dittmer, U., Meyer, D., Langergraber, G. (2005): Simulation of a Subsurface Vertical Flow Constructed Wetland for CSO Treatment. *Water Sci Technol* 51(9), 225-232.

Faulwetter, J.L., Gagnon, V., Sundberg, C., Chazarenc, F., Burr, M.D., Brisson, J., Camper, A.K., Stein, O.R. (2009): Microbial processes influencing performance of treatment wetlands: A review. *Ecol Eng* 35, 987-1004.

Forquet, N., Wanko, A., Mosé, R., Sadowski, A.-G. (2009): Diphasic modelling of vertical flow filter. *Ecol Eng* 35(1), 47-56.

Freire, F.G., Davies, L.C., Vacas, A.M., Novais, J.M., Martins-Dias, S. (2009): Influence of operating conditions on the degradation kinetics of an azo-dye in a vertical flow constructed wetland using a simple mechanistic model. *Ecol Eng* 35(10), 1379-1386.

Giraldi, D., de'Michieli Vitturi, M., Iannelli, R. (2010): FITOVERT: a dynamic numerical model of subsurface vertical flow constructed wetlands. *Environ Model Softw* 25, 633–640.

Headley, T., Herity, E., Davison, L. (2005): Treatment at different depths and vertical mixing within a 1-m deep horizontal subsurface-flow wetland. *Ecol Eng* 25(5), 567-582.

Henrichs, M., Langergraber, G., Uhl, M. (2007): Modelling of organic matter degradation in constructed wetlands for treatment of combined sewer overflow. *Sci Total Environ* 380(1-3), 196-209.

Henrichs, M., Welker, A., Uhl, M. (2009): Modelling of biofilters for ammonium reduction in combined sewer overflow. *Water Sci Technol* 60(3), 825-831.

Henze, M., Gujer, W., Mino, T., van Loosdrecht, M.C.M. (2000): Activated sludge models ASM1, ASM2, ASM2D and ASM3. *IWA Scientific and Technical Report No.9*, IWA Publishing, London, UK.

Kadlec, R., Wallace, S. (2009): Treatment Wetlands. 2nd edition, CRC press, Boca Raton, FL, USA.

Langergraber, G. (2001): Development of a simulation tool for subsurface flow constructed wetlands. *Wiener Mitteilungen* 169, Vienna, Austria, 207p (ISBN 3-85234-060-8).

Langergraber, G. (2007): Simulation of the treatment performance of outdoor subsurface flow constructed wetlands in temperate climates. *Sci Total Environ* 380(1-3), 210-219.

Langergraber, G. (2008): Modeling of processes in subsurface flow constructed wetlands – A review. *Vadoze Zone J* 7(2), 830-842.

Langergraber, G. (2010): Process based models for subsurface flow constructed wetlands. In: Vymazal, J. (ed.): "*Water and Nutrient Management in Natural and Constructed Wetlands*", Springer Science + Business Media B.V., Dordrecht Heidelberg London New York, pp.21-36 (ISBN 978-90-481-9584-8).

Langergraber, G. (2011): Numerical modelling: A tool for better constructed wetland design? *Water Sci Technol*, accepted for publication.

Langergraber, G., Šimůnek, J. (2005): Modeling variably-saturated water flow and multi-component reactive transport in constructed wetlands. *Vadose Zone J* 4(4), 924-938.

Langergraber, G., Šimůnek, J. (2006): The multi-component reactive transport module CW2D for constructed wetlands for the HYDRUS Software Package. *HYDRUS Software Series 2*, Department of Environmental Sciences, University of California Riverside, Riverside, CA, USA, 72p.

Langergraber, G., Giraldi, D., Mena, J., Meyer, D., Peña, M., Toscano, A., Brovelli, A, Korkusuz, E.A. (2009a): Recent developments in numerical modelling of subsurface flow constructed wetlands. *Sci Total Environ* 407(13), 3931-3943.

Langergraber, G., Rousseau, D., García, J., Mena, J. (2009b): CWM1 - A general model to describe biokinetic processes in subsurface flow constructed wetlands. *Water Sci Technol* 59(9), 1687-1697.

Langergraber, G., Tietz, A., Haberl, R. (2007): Comparison of measured and simulated distribution of microbial biomass in subsurface vertical flow constructed wetlands. *Water Sci Technol* 56(3), 233-240.

Maier, U., DeBiase, C., Baeder-Bederski, O., Bayer, P. (2009): Calibration of hydraulic parameters for large-scale vertical flow constructed wetlands. *J Hydrol* 369, 260–273.

Marsili-Libelli, S., Checchi N..(2005): Identification of dynamic models for horizontal subsurface constructed wetlands. *Ecol Model* 187(2-3), 201-218.

Mashauri, D.A., Kayombo. S. (2002): Application of the two coupled models for water quality management: facultative pond cum constructed wetland models. *Phys Chem Earth* 27(11-12), 773–781.

Mayo, A.W., Bigambo. T. (2005): Nitrogen transformation in horizontal subsurface flow constructed wetlands I: Model development. *Phys Chem Earth* 30(11-16), 658-667

McGechan, M.B., Moir, S.E., Castle, K., Smit, I.P.J. (2005): Modelling Oxygen Transport in a Reedbed-constructed Wetland Purification System for Dilute Effluents. *Biosyst Eng* 91(2), 191-200.

Meyer, D., Dittmer, U., Schmitt, T.G. (2008): Modelling CWs for CSO treatment-reasonable balancing between detailed description and practicable handling. In: IWA (eds., 2008): *Proceedings of the 11th IWA Specialized Group Conference on "Wetland Systems for Water Pollution Control"* - Volume 2, 1-7 November 2008, Indore, India, pp.851-857.

Ojeda E., Caldentey, J., Saaltink, M.W., García, J. (2008): Evaluation of relative importance of different microbial reactions on organic matter removal in horizontal subsurface-flow constructed wetlands using a 2D simulation model. *Ecol Eng* 34(1), 65-75.

Rousseau, D.P.L. (2005): Performance of constructed treatment wetlands: model-based evaluation and impact of operation and maintenance. *PhD thesis*, Ghent University, Belgium.

Schwager, A., Boller, M. (1997): Transport phenomena in intermittent filters. *Water Sci Technol* 35(6), 13-20.

Šimůnek, J., van Genuchten, M.Th., Šejna, M. (2008): Development and applications of the HYDRUS and STANMOD software packages and related codes, *Vadose Zone J 7*(2), 587-600.

Šimůnek J., Šejna, M., van Genuchten, M.Th. (2011): The HYDRUS Software Package for Simulating the Two- and Three-Dimensional Movement of Water, Heat, and Multiple Solutes in Variably-Saturated Media. *Technical Manual*, Version 2.0. PC-Progress, Prague, Czech Republic, 254p.

Smethurst, P.J., Petrone, K.C., Baillie, C.C., Worledge, D., Langergraber, G. (2010): Streamside management zones for buffering streams on farms: Observations and nitrate modelling. Final project report, CSIRO, Hamilton, TA, Australia.

Smethurst, P.J., Langergraber, G., Petrone, K.C., Holz, G. (2009): Hillslope and stream connectivity: simulation of concentration-discharge patterns using the HYDRUS model. In: Proceedings 18th World IMACS Congress and MODSIM09 International Congress on Modelling and Simulation, 13–17 July 2009, Cairns, Australia, pp.4057-4063 (http://www.mssanz.org.au/modsim09/I14/smethurst_I14.pdf).

Toscano, A., Langergraber, G., Consoli, S., Cirelli, G.L. (2009): Modelling pollutant removal in a pilot-scale two-stage subsurface flow constructed wetlands. *Ecol Eng* 35(2), 281-289.

Wang, Y., Zhang, J., Kong, H., Inamori, Y., Xu, K., Inamori, R., Kondo, T. (2009): A simulation model of nitrogen transformation in reed constructed wetlands. *Desalination* 235(1-3), 93-101.

Wanko, A., Mose, R., Carrayrou, J., Sadowski, A.G. (2006): Simulation of Biodegradation in Infiltration Seepage - Model Development and Hydrodynamic Calibration. *Water Air Soil Poll* 177, 19–43.

Wynn, M.T., Liehr. S.K. (2001): Development of a constructed subsurface-flow wetland simulation model. *Ecol Eng* 16, 519-536.